bioRxiv preprint doi: https://doi.org/10.1101/2021.07.22.453263; this version posted July 22, 2021. The copyright holder for this preprint (which was not certified by peer review) is the author/funder, who has granted bioRxiv a license to display the preprint in perpetuity. It is made available under aCC-BY 4.0 International license.

Gammaherpesvirus infection licenses age-associated B cells for pathogenicity in MS and EAE

Isobel C. Mouat[1], Jessica R. Allanach[1], Vina Fan[1,2], Anna M. Girard[1,2], Iryna Shanina[1], Galina Vorobeychik[3,4], and Marc S. Horwitz[1]

[1] Department of Microbiology and Immunology, University of British Columbia, Vancouver, British Columbia, Canada

[2] Department of Medicine, University of Calgary, Calgary, Alberta, Canada

[3] Fraser Health Multiple Sclerosis Clinic, Burnaby, British Columbia, Canada

[4] Division of Neurology, Department of Medicine, University of British Columbia, Vancouver British Columbia, Canada

Corresponding author:

Marc S. Horwitz

Room 3551, Life Sciences Centre

2350 Health Sciences Mall

University of British Columbia

Vancouver, B. C. Canada V6T 1Z3

604-822-6298

mhorwitz@mail.ubc.ca

bioRxiv preprint doi: https://doi.org/10.1101/2021.07.22.453263; this version posted July 22, 2021. The copyright holder for this preprint (which was not certified by peer review) is the author/funder, who has granted bioRxiv a license to display the preprint in perpetuity. It is made available under aCC-BY 4.0 International license.

Abstract

While age-associated B cells (ABCs) are known to expand and persist following viral infection and during autoimmunity, their interactions are yet to be studied together in these contexts. Epstein-Barr virus (EBV) infection has long been implicated in multiple sclerosis (MS), and it is not known whether ABCs could play a role in mediating viral contribution to autoimmunity. Here, we show that the circulating ABC population is expanded in people with MS and that EBV infection and MS status differentially impact the circulating ABC phenotype. We then directly compared ABCs during viral infection and autoimmunity using mouse models of EBV, gammaherpesvirus 68 (γHV68), and MS, experimental autoimmune encephalomyelitis (EAE). We observed that splenic ABCs are expanded in a sex-biased manner during both latent virus infection and EAE, and each event drives the ABC population to opposing phenotypes. We have previously shown that latent γHV68 infection exacerbates EAE and here we show that mice lacking ABCs fail to display γHV68-enhanced disease. Collectively, these findings indicate that latent viral infection and central nervous system autoimmunity differentially impact the ABC population and suggests that viral infections such as EBV prime ABCs to contribute pathogenically in MS.

Conflict of interest statement

The authors have declared that no conflict of interest exists.

bioRxiv preprint doi: https://doi.org/10.1101/2021.07.22.453263; this version posted July 22, 2021. The copyright holder for this preprint (which was not certified by peer review) is the author/funder, who has granted bioRxiv a license to display the preprint in perpetuity. It is made available under aCC-BY 4.0 International license.

Introduction

Age-associated B cells (ABCs) are a unique subset of immune B cells found in humans and mice. They have been identified and characterized independently in the contexts of female aging, viral infection, and autoimmunity(1–3). In life, these are overlapping and intertwined occurrences. In this study, we show that viral infection and autoimmunity differentially impact the phenotype of ABCs in humans and mice, and we identify ABCs as functional mediators of viral-enhanced autoimmunity.

ABCs, defined by high expression of CD11c and T-bet and low expression of CD21, are primarily found in the spleen and secrete antiviral or auto-antibodies, cytokines, and act as potent antigen-presenting cells(1,4,5). The number of ABCs increases with age, particularly in females(3,6–10). ABC numbers are also increased in people with autoimmune diseases, including systemic lupus erythematosus (SLE), rheumatoid arthritis (RA), individuals with multiple sclerosis (MS) over 60 years of age, and a subset of people with common variable immunodeficiency that display autoimmune complications(3,6,7,9–11). In a mouse model of SLE, knocking out T-bet specifically in B cells impairs the development of germinal centers, decreases autoantibody levels, and dampens kidney damage and mortality(12). ABCs have been shown to produce proinflammatory cytokines IFNγ and TNFα as well as regulatory cytokine IL-10 in autoimmune contexts(4,13). To our knowledge, ABCs have yet to be examined in the in vivo MS-model experimental autoimmune encephalomyelitis (EAE), though ABC differentiation depends on T-bet, a transcription factor that is essential for EAE(14). The functional capacities of ABCs and their contribution(s) to MS and EAE are not well understood. ABCs also expand in an array of viral infections including lymphocytic choriomeningitis virus (LCMV), murine

bioRxiv preprint doi: https://doi.org/10.1101/2021.07.22.453263; this version posted July 22, 2021. The copyright holder for this preprint (which was not certified by peer review) is the author/funder, who has granted bioRxiv a license to display the preprint in perpetuity. It is made available under aCC-BY 4.0 International license.

cytomegalovirus (MCMV), gammaherpesvirus68 (γHV68), vaccinia, human immunodeficiency virus (HIV), influenza, hepatitis C, and rhinovirus(15–22). ABCs have primarily been examined separately in the contexts of viral infection and autoimmunity. Given the distinct environments of viral infection and autoimmunity, it would be predicted that ABCs would take on distinct phenotypes and functional capacities. Recently, ABCs in people with HIV and SLE were shown to have similar but not completely overlapping transcriptional profiles(23). The phenotypic and functional characteristics of ABCs between disease states deserves further investigation.

Here, we do a side-by-side comparison of the ABC population in the contexts of both viral infection and autoimmunity in both humans and mice to ascertain the specific interactions driven by these two processes and their relative role in disease progression. We also examine the role of ABCs as mediators between gammaherpesvirus infection and MS/EAE. Epstein-Barr virus (EBV) is a highly prevalent virus, infecting over 90% of the adult human population(24). The association between EBV and autoimmunity was first demonstrated in 1979 when it was reported that peripheral blood lymphocytes from MS patients have an increased tendency to transform in vitro in response to EBV(25). Clinical findings support the association between EBV and MS: people with MS have higher titres of EBV-specific antibodies than healthy individuals(26) which correlate with disease activity(27), and T cells in people with MS display aberrant responses to EBV(28). Further work has demonstrated that EBV's association with autoimmune disease extends to SLE and RA(29–34). The precise mechanism of EBV's contribution to MS is controversial – EBV-infection of autoreactive B cells, molecular mimicry, bystander activation of autoreactive cells, EBV-infected B cell invasion of the central nervous

bioRxiv preprint doi: https://doi.org/10.1101/2021.07.22.453263; this version posted July 22, 2021. The copyright holder for this preprint (which was not certified by peer review) is the author/funder, who has granted bioRxiv a license to display the preprint in perpetuity. It is made available under aCC-BY 4.0 International license.

84 system (CNS) and activation of Human Endogenous Retrovirus-W, and EBV-induced cytokine
85 response have all been suggested(35,36).

86 Our group has previously demonstrated that infection with latent γHV68, a murine
87 model of EBV(37), exacerbates MOG_{35-55} EAE in C57BL/6(J) mice(38). Mice latently infected with
88 γHV68 display an earlier and more severe EAE clinical course without viral reactivation or CNS
89 infection. Latently γHV68-infected mice have a heightened peripheral cytotoxic T cell response
90 and develop CNS lesions composed of $CD4^+$ and $CD8^+$ T cells, with a proportion of infiltrating
91 $CD8^+$ T cells specific for γHV68. Disease enhancement is dependent on the development of
92 latency and is specific to γHV68; other viral infections including LCMV and MCMV do not lead to
93 EAE enhancement(39). This γHV68-EAE model is a valuable model of the relationship between
94 EBV and MS and here, we demonstrate that the specific induction of ABCs is required for the
95 latent γHV68-enhancement of EAE.

96 In this study, we directly compare the ABC population in the contexts of both latent viral
97 infection and autoimmunity in humans and mice and distinguish the role of ABCs between
98 different models of CNS autoimmunity, EAE and latent γHV68 enhancement of EAE. We
99 propose that alteration of the ABC population due to gammaherpesvirus infection is a
100 mechanism by which viral infection contributes to the development and progression of
101 autoimmune disease.

bioRxiv preprint doi: https://doi.org/10.1101/2021.07.22.453263; this version posted July 22, 2021. The copyright holder for this preprint (which was not certified by peer review) is the author/funder, who has granted bioRxiv a license to display the preprint in perpetuity. It is made available under aCC-BY 4.0 International license.

Results

EBV and MS status alter the circulating ABC population

We first compared the ABC population frequency and phenotype in individuals with and without a history of EBV infection and MS. Peripheral blood mononuclear cells (PBMCs) were collected from EBV^- and EBV^+ healthy women and people with MS, all of whom are EBV^+ women, and the ABC proportion and phenotype were examined by flow cytometry. The people diagnosed with MS were not exposed to immunomodulatory treatments and had disease durations ranging from 4 months to 7 years (**Table 1**). All donors were female and median ages between groups were comparable: EBV^- healthy donors (25 years), EBV^+ healthy donors (26.5 years), and EBV^+ people with MS (31 years) (**Table 1**). EBV and CMV serostatus was determined by ELISA.

For this study, ABCs were defined as $CD19^+CD20^+CD11c^+CD21^-$ (**Figure 1A**). Gene analysis has shown $CD19^+CD21^-$ B cells display high levels of CD11c and express T-bet(7,40). Further, CD11c and CD21 have been used by other groups to define ABCs in people(3,6). Only extracellular staining was performed to preserve cell numbers due to low prevalence of ABCs.

We found that people with MS have increased proportions of circulating ABCs compared to EBV seronegative healthy people (**Figure 1B**). EBV seropositive healthy individuals show a nonsignificant trend towards increased ABC proportions compared to EBV seronegative healthy people but reduced compared to MS (**Figure 1B**). Among the donor groups, we do not observe differences in the proportion of total circulating B cells (**Supplementary Figure 1A**). These findings indicate that both EBV infection and MS might expand the proportion of

bioRxiv preprint doi: https://doi.org/10.1101/2021.07.22.453263; this version posted July 22, 2021. The copyright holder for this preprint (which was not certified by peer review) is the author/funder, who has granted bioRxiv a license to display the preprint in perpetuity. It is made available under aCC-BY 4.0 International license.

123 circulating ABCs. In addition to changes to ABC proportions, we also observe differences in ABC
124 phenotype between groups.

125 We examined the impact of EBV infection and MS on the ABC phenotype, because the
126 impact of autoimmunity versus viral infection on the ABC phenotype has not been thoroughly
127 studied. For these purposes, our preliminary analysis focused on the proportion of ABCs
128 expressing Fas, PD1, and CD27. ABCs have previously been shown to express substantially more
129 Fas than non-ABC B cells(3,40) and ABCs in people with common variable immune deficiency
130 express more Fas than ABCs in healthy donors(9). Another inhibitory receptor, PD1, has also
131 been shown to be upregulated on ABCs compared to other B cell subsets both in healthy
132 individuals and those with SLE(10,16). The role of CD27, a marker of memory, on ABCs is not
133 well understood – ABCs have been reported to express high CD27(3), though some groups
134 define ABCs as CD27 negative(16,40). It is not known how infection versus autoimmunity
135 impact the expression of Fas, PD1, and CD27 on ABCs. We observed that slightly over half of
136 ABCs express Fas, and EBV infection led to a nonsignificant increase in the proportion of ABCs
137 positive for Fas compared to EBV seronegative healthy individuals (**Figure 1C**). Among people
138 who are EBV seropositive, MS led to a significant decrease in the proportion of ABCs expressing
139 Fas compared to healthy donors (**Figure 1C**). In contrast to previous reports(10,16), we found
140 that a low proportion of ABCs express PD1 and the proportion of ABCs that express PD1 is not
141 different across EBV seronegative or EBV seropositive healthy individuals or people with MS
142 (**Figure 1D**). Finally, just under half of ABCs express CD27, and EBV and MS status did not impact
143 the proportion of ABCs that express CD27 (**Figure 1E**).

144 We observed that CMV status did not significantly correlate with the ABC phenotype in

bioRxiv preprint doi: https://doi.org/10.1101/2021.07.22.453263; this version posted July 22, 2021. The copyright holder for this preprint (which was not certified by peer review) is the author/funder, who has granted bioRxiv a license to display the preprint in perpetuity. It is made available under aCC-BY 4.0 International license.

145 healthy individuals nor those with MS (**Supplemental Figure 1**), indicating that CMV, another
146 herpesvirus linked to MS, may be less influential of this B cell population compared to EBV. To
147 further investigate how ABCs differ between the contexts of viral infection and MS, and
148 whether ABCs can act as mediators of the viral contribution to disease, we investigated in vivo
149 models of infection and disease.

Age at donation (years)	Country of birth and age of immigration to Canada (if applicable)	Self-identified ethnicity (boxes checked)	Age (years) at MS symptom onset	EDSS score at time of donation	Disease duration at time of donation	EBV status	CMV status
25	Country: Canada Age: N/A	Canadian	23	2.0	2 years 8 months	VCA+, EBNA-1+	-
24	Country: United Kingdom Age: 5 years	Middle Eastern	24	2.5	4 months	VCA+, EBNA-1+	+
31	Country: Afghanistan Age: 20 years	Middle Eastern	31	2.5	6 months	VCA+, EBNA-1-	+
32	Country: Canada Age: N/A	Canadian	26	2.0	5 years	VCA+, EBNA-1+	-
39	Country: Canada Age: N/A	Canadian, English, Scottish, Irish	31	2.0	7 years	VCA+, EBNA-1+	-
25	Country: Canada Age: N/A	Canadian, English	N/A	N/A	N/A	VCA-EBVNA1-	-
26	Country: Canada Age: N/A	Canadian	N/A	N/A	N/A	VCA-EBVNA1-	-
18	Country: Canada Age: N/A	Canadian, Chinese	N/A	N/A	N/A	VCA-EBVNA1-	+
39	Country: Canada Age: N/A	Canadian	N/A	N/A	N/A	VCA+ EBNA1+	-
23	Country: Canada Age: N/A	Canadian, Scottish	N/A	N/A	N/A	VCA+ EBNA1+	+
25	Country: Canada Age: N/A	Canadian, Scottish, Swedish, First Nations	N/A	N/A	N/A	VCA+ EBNA1-	+
28	Country: Canada Age: N/A	Canadian, Dutch	N/A	N/A	N/A	VCA+ EBNA1+	-

150

151 **Table 1:** Donor characteristics.

bioRxiv preprint doi: https://doi.org/10.1101/2021.07.22.453263; this version posted July 22, 2021. The copyright holder for this preprint (which was not certified by peer review) is the author/funder, who has granted bioRxiv a license to display the preprint in perpetuity. It is made available under aCC-BY 4.0 International license.

γHV68 infection and EAE induction increase ABCs

To determine whether ABCs are differentially impacted by gammaherpesvirus infection and an in vivo model of MS, we examined the proportion of ABCs following latent γHV68 infection and EAE induction. We examined the relative proportions of ABCs in C57BL/6(J) mice mock-infected (naïve), infected i.p. with 10^4 PFU γHV68 for 35 days to establish latency (γHV68), induced with EAE (MOG_{35-55} with pertussis toxin on day 0 and 2 post-induction) for 12-14 days (EAE), or infected with γHV68 for 35 days, then induced for MOG_{35-55} EAE for 12-14 days (γHV68-EAE). We collected spleens, brains, and spinal cords, processed for, and performed flow cytometry to examine ABCs (**Supplemental Figure 2A**). We asked whether the abundance of ABCs in the spleen changes with γHV68 infection, EAE induction, or both, and whether ABCs are found at the site of disease, the CNS, during EAE.

We found that ABCs expand in the spleen in a sex-biased manner during γHV68 infection and EAE. While γHV68 infection increases the relative proportion of ABCs among mature B cells in the spleen in both male and female mice, induction of EAE increases the proportion of ABCs only in females (**Figure 2A-B**). During γHV68-EAE, the proportion of ABCs are increased compared to naïve mice in both females and males (**Figure 2A-B**). The proportion of ABCs is increased in females as compared to males in γHV68, EAE, and γHV68-EAE mice, though there is no sex bias observed in naïve mice (**Figure 2C-F**). We did not observe a difference in T-bet expression in splenic ABCs between groups (**Supplemental Figure 2B**). Due to the observed sex bias, we focused our analysis on female mice.

We asked whether γHV68-infection or EAE leads changes ABC numbers in the CNS, the site of disease during EAE. Not surprisingly, under control conditions where CNS infiltration

bioRxiv preprint doi: https://doi.org/10.1101/2021.07.22.453263; this version posted July 22, 2021. The copyright holder for this preprint (which was not certified by peer review) is the author/funder, who has granted bioRxiv a license to display the preprint in perpetuity. It is made available under aCC-BY 4.0 International license.

174 does not occur, specifically, γHV68 infection alone and without EAE induction, did not result in
175 increased numbers of ABCs in the brain or spinal cord (**Figure 2G-H**). However, EAE induction
176 increased the number of ABCs in the brain and spinal cord in both uninfected and γHV68-
177 infected mice (**Figure 2G-H**). Unlike the spleen, we did not observe a sex difference in the
178 number of ABCs within the CNS (**Supplemental Figure 2C-D**). We found that ABCs constitute a
179 lower proportion of total lymphocytes in the brain and spinal cord compared to the spleen
180 (**Supplemental Figure 2E**), indicating that they are likely not preferentially homing to the CNS
181 during disease. The precise localization of the CNS-infiltrating ABCs is not known, and whether
182 they localize in the meninges, parenchyma, or associate with lesions or ectopic lymphoid
183 structures, could give insight into their role within the CNS during disease.

184 These findings demonstrate that ABCs display a sex bias in the contexts of viral infection
185 and autoimmunity and support previous findings that ABCs are largely resident in the spleen.
186 To further investigate the role(s) of ABCs in viral infection and autoimmunity, we next examined
187 the phenotype of ABCs in these different contexts.

188 ## γHV68 infection and EAE differentially impact ABC phenotype

189 Although ABCs are implicated in both viral infection and autoimmunity, to our knowledge the
190 ABC phenotype has not been directly examined in these two instances. To compare how γHV68
191 infection and EAE induction influence the ABC phenotype, we used flow cytometry to examine
192 extracellular and intracellular antigens on splenic ABCs to compare the phenotype of ABCs
193 specifically in EAE with and without prior γHV68 infection. We found that γHV68 infection and
194 EAE drive differential ABC phenotypes that are distinct from each other and the ABC phenotype
195 of naïve mice. Specifically, γHV68 infection led to an increase in the proportion of ABCs

bioRxiv preprint doi: https://doi.org/10.1101/2021.07.22.453263; this version posted July 22, 2021. The copyright holder for this preprint (which was not certified by peer review) is the author/funder, who has granted bioRxiv a license to display the preprint in perpetuity. It is made available under aCC-BY 4.0 International license.

196 expressing IFNγ and TNFα, and a decrease in ABCs expressing IL-17A (**Figure 3A, Supplemental**
197 **Figure 3A-C**). In contrast, EAE results in an increased proportion of ABCs expressing IL-17A and
198 IL-10, and no change in IFNγ or TNFα, compared to ABCs in naïve mice (**Figure 3A,**
199 **Supplemental Figure 3A-C**).

200 Further, γHV68 infection results in significantly fewer ABCs expressing the inhibitory
201 receptors CTLA4, PDL1, and IDO, while EAE increases the proportion of ABCs expressing CTLA4,
202 PD1, and PDL1 (**Figure 3A, Supplemental Figure 3E-H**). The proportion of ABC expressing Fas
203 appeared unchanged by γHV68 infection or EAE (**Figure 3A, Supplemental Figure 3I**). γHV68
204 infection increased the proportion of ABCs expressing the memory marker CD27, while EAE did
205 not (**Figure 3A, Supplemental Figure 3J**).

206 We asked how γHV68 infection prior to EAE induction impacts the phenotype of ABCs.
207 We observed that the ABCs in γHV68-EAE mice display an intermediate phenotype between
208 those of γHV68 and EAE mice. In particular, the proportion of ABCs in γHV68-EAE mice positive
209 for cytokines IL-17A, IFNγ, and IL-10 is intermediate between those of γHV68 and EAE mice
210 (**Figure 3B-C, Supplemental Figure 3A, C, D**). In addition, an intermediate amount of the ABCs
211 in γHV68-EAE mice expressed inhibitory receptors CTLA4, PDL1, PD1, and IDO between those in
212 γHV68 and EAE (**Supplemental Figure 3E-H**). This intermediate phenotype displayed by ABCs in
213 γHV68-EAE mice appeared to be more pathogenic than the ABC phenotype in uninfected EAE
214 mice. We found that ABCs in γHV68-EAE mice express more IFNγ and less IL-17A than ABCs in
215 EAE mice (**Figure 3D-E, Supplemental Figure 3A, C**), indicating that ABCs in γHV68-EAE mice
216 display a more Th-1 associated phenotype than those in EAE mice. We detected no difference
217 in the proportion of ABCs expressing IL-10 or TNFα between EAE and γHV68-EAE mice, though

bioRxiv preprint doi: https://doi.org/10.1101/2021.07.22.453263; this version posted July 22, 2021. The copyright holder for this preprint (which was not certified by peer review) is the author/funder, who has granted bioRxiv a license to display the preprint in perpetuity. It is made available under aCC-BY 4.0 International license.

ABCs in γHV68-EAE express less PD1 and more CD27 (**Figure 3F-I, Supplemental Figure 3G, J**). As we have previously shown that γHV68-exacerbation of EAE is associated with a robust Th-1 response, in both the periphery and CNS, the presence of the Th-1 like ABC phenotype suggested that γHV68-primed ABCs could contribute to the exacerbation of EAE disease.

ABC knockout mice demonstrate that ABCs are protective in EAE and pathogenic in γHV68-EAE

Next, we sought to determine whether ABCs contribute to the EAE or γHV68-EAE clinical course. Previously, our lab has shown that latent γHV68 infection prior to disease induction results in an exacerbated clinical course, with a Th-1 skewed immune response and increased CD8 T cell infiltration to the CNS(38).

To investigate the role of ABCs in disease we examined mice with a B cell specific T-bet deletion(12) that lack ABCs. We demonstrate a significant loss of ABCs in *Tbx21*$^{fl/fl}$*Cd19*$^{cre/+}$ (KO) compared to *Tbx21*$^{fl/fl}$*Cd19*$^{+/+}$ (Ctrl) littermate controls (**Figure 4A**). Female Ctrl and KO mice were mock-infected or infected with γHV68 for 35 days and induced for MOG_{35-55} EAE. Mice were monitored daily post EAE-induction, blinded to genotype, and measured on a 5-point scale as previously described(38).

Strikingly, we observed that mice lacking ABCs had the opposite effect on the clinical course of EAE and γHV68-EAE. Specifically, during EAE ABC KO mice developed more severe disease than Ctrl mice, while in γHV68-EAE, the disease course was less severe than Ctrl mice (**Figure 4B-D**). During EAE, KO mice displayed an earlier day of onset, and higher cumulative and endpoint scores than Ctrl mice (**Figure 4E-G**). In contrast, γHV68-EAE KO mice displayed a lower endpoint score (**Figure 4G**).

These results indicate that ABCs contribute protectively in EAE and pathogenically in

bioRxiv preprint doi: https://doi.org/10.1101/2021.07.22.453263; this version posted July 22, 2021. The copyright holder for this preprint (which was not certified by peer review) is the author/funder, who has granted bioRxiv a license to display the preprint in perpetuity. It is made available under aCC-BY 4.0 International license.

γHV68-EAE and these results align with our prior observations that ABCs display a more pathogenic phenotype in γHV68-EAE, compared to EAE. In addition, while in Ctrl mice γHV68-EAE resulted in an exacerbated disease course compared to EAE alone, ABC KO mice did not display enhanced CNS disease thereby demonstrating that ABCs are required for γHV68-enhancement of EAE.

Knocking out ABCs impacts the T cell population but not autoantibodies

ABCs are major producers of IgG2a/c(18,41) and, in a model of SLE, knocking out ABCs results in a significant decrease in anti-chromatin IgG2a/c titres(12). To ask whether autoantibodies were mechanistically responsible for the impact in disease observed here, we analyzed the sera from these mice. Surprisingly, we did not observe differences in anti-MOG IgG2a/c titres between Ctrl and KO mice during EAE and γHV68-EAE (**Figure 5A-B**), indicating that, in this context, ABCs are contributing to disease via a mechanism other than autoantibody production.

It is known that ABCs are capable of presenting antigen(5) and we and others see that ABCs are predominantly spleen-resident(17). Therefore, we speculated that ABCs could impact T cell polarization in the spleen and infiltration of the CNS. In the spleen there is no difference in the proportion of cytotoxic or helper T cells between Ctrl and KO mice during EAE or γHV68-EAE (**Supplemental Figure 4A-B**). However, the skewing of the peripheral T cells is altered in KO mice during γHV68-EAE. During γHV68-EAE, KO mice did not display the increase in IFNγ-expressing CD4 or CD8 T cells in the spleen that is seen in Ctrl mice (**Figure 5C-D**). Additionally, significantly fewer helper T cells express IL-17A in KO mice during γHV68-EAE compared to Ctrl mice(**Figure 5E**). The decrease in proportion of $IFN\gamma^+$ and $IL\text{-}17A^+$ T cells in KO mice during γHV68-EAE could explain the dampened disease course in these mice. In addition, there were

bioRxiv preprint doi: https://doi.org/10.1101/2021.07.22.453263; this version posted July 22, 2021. The copyright holder for this preprint (which was not certified by peer review) is the author/funder, who has granted bioRxiv a license to display the preprint in perpetuity. It is made available under aCC-BY 4.0 International license.

proportionately fewer CD4 T cells expressing IL-10 in KO mice during γHV68-EAE (**Supplemental Figure 4C**). The decrease in proportion of T cells expressing IFNγ and IL-17A and increase in IL-10 likely indicates that, without ABCs, the peripheral immune response is shifting towards a tolerogenic state. KO mice in both EAE and γHV68-EAE displayed a trend of increased regulatory T cells in the spleen, indicating that ABCs may dampen the regulatory T cell population (**Figure 5F**).

In contrast to γHV68-EAE mice, there were no changes in splenic T cell skewing during EAE between Ctrl and KO mice (**Figure 5C-D**). In EAE mice, the proportion of cytotoxic and helper T cells, and the proportion of CD4 T cells expressing IFNγ, IL-17A, and IL-10 did not differ between Ctrl and KO mice (**Figure 5C-E, Supplemental Figure 4A-C**). These results indicate that ABCs impact T cell skewing in the spleen during γHV68-EAE, though not EAE.

In EAE mice, although we did not observe major differences in the periphery between Ctrl and KO mice, there were significant differences in CNS lymphocyte infiltration. KO mice induced for EAE displayed increased numbers of lymphocytes infiltrating the spinal cord, where disease predominates, compared to Ctrl (**Figure 5G**). This indicates that rather than impacting T cell skewing in the periphery, ABCs in EAE mice could possibly be influencing CNS lymphocyte homing or blood-brain barrier integrity, yet there was no significant difference in CNS-infiltrating lymphocytes in γHV68-EAE (**Figure 5G-H**). Further, there were no significant differences in the number of cytotoxic, helper, or regulatory T cells infiltrating the CNS between Ctrl and KO mice during EAE or γHV68-EAE (**Supplemental Figure 4D-I**). While eliminating some cell types, these results beg further analysis to understanding the cell populations that are

bioRxiv preprint doi: https://doi.org/10.1101/2021.07.22.453263; this version posted July 22, 2021. The copyright holder for this preprint (which was not certified by peer review) is the author/funder, who has granted bioRxiv a license to display the preprint in perpetuity. It is made available under aCC-BY 4.0 International license.

283 infiltrating the CNS in KO mice during EAE.

284 Prior work had shown that specifically deleting T-bet from B cells lead to an inability of
285 mice to control LCMV chronic infection(18,41). To test the impact of γHV68 replication, we
286 found an increased quantity of γHV68 in the spleen of ABC KO mice compared to Ctrl during
287 γHV68-EAE (**Supplemental Figure 4J**). The ability of ABCs to control γHV68 load and the clinical
288 course of disease warrants further investigation.

289 Together, these findings indicate that ABCs influence T cell skewing in the periphery and
290 lymphocyte infiltration of the CNS during disease. The precise mechanisms by which ABCs
291 impact T cell skewing and lymphocyte migration to and infiltration of the CNS warrants further
292 investigation.

293 ## Discussion

294 In this report, we have shown that that age-associated B cell population is differentially
295 impacted by viral infection and autoimmunity, in both mice and humans. We have sought to
296 directly compare the ABC population in these two contexts and examine ABCs in conditions of
297 combined latent viral infection and autoimmunity, which is relevant to MS patients. In addition,
298 we examined the functional contribution of ABCs and identified them as a mediator between
299 latent gammaherpesvirus and MS disease.

300 Together, these findings indicate that ABCs are differentially impacted by viral infection
301 and autoimmunity, in both mice and people. Additionally, we found that ABCs in γHV68-EAE
302 mice take on a phenotype with characteristics of both the viral infection and disease,
303 demonstrating that ABCs are a heterogeneous population, at least phenotypically, particularly
304 when challenged by multiple antigens. These findings have implications for studying the human

bioRxiv preprint doi: https://doi.org/10.1101/2021.07.22.453263; this version posted July 22, 2021. The copyright holder for this preprint (which was not certified by peer review) is the author/funder, who has granted bioRxiv a license to display the preprint in perpetuity. It is made available under aCC-BY 4.0 International license.

ABC population that is undoubtedly impacted by an array of pathogens and contexts.

A surprising finding of this study was the female sex bias of ABCs in mice infected with γHV68 and/or induced for EAE. This finding is relevant to the question of if ABCs play a role in the sex-bias observed in various autoimmune diseases, including MS and SLE, as has previously been suggested(42). Interestingly, MOG_{35-55} EAE does not display a sex bias in C57BL/6 mice(43,44), so if and how the increased numbers of ABCs in female EAE mice impact disease in this model remains unknown.

We observed that the ABC phenotype is differentially impacted by viral infection and autoimmunity in mice and humans, though the phenotype observed in mice and humans does not always align. For instance, we observe that the proportion of ABCs that express Fas is decreased in people with MS compared to healthy EBV^+ donors, while in mice we observe an increase in γHV68-EAE compared with γHV68. This disconnect between the mouse and human ABC phenotype may be due to intrinsic differences between the immune systems in mice and humans or the lack of previous antigen exposure in the mice. Additionally, it must be considered whether circulating ABCs are representative of those in the spleen. We and others observed that ABCs are predominantly spleen-resident in mice(17), and further investigation should examine ABCs in the spleen versus circulation, especially because most human samples examined are blood.

We also found that ABCs are heterogenous in terms of phenotype and functional capacity depending on context and can contribute to disease in a protective or pathogenic manner. ABCs likely comprise several subsets that differ in terms of functional capacity. In the future, it will be important to determine disease-associated subsets; a portion of ABCs could

bioRxiv preprint doi: https://doi.org/10.1101/2021.07.22.453263; this version posted July 22, 2021. The copyright holder for this preprint (which was not certified by peer review) is the author/funder, who has granted bioRxiv a license to display the preprint in perpetuity. It is made available under aCC-BY 4.0 International license.

contribute to disease, and others act in a regulatory/protective manner. An outstanding question is whether the ABCs population is effectively depleted by Rituximab, and if the ABC population is affected by other immunomodulatory treatments.

Interestingly, it appears that ABCs contribute to some models of autoimmunity in a protective manner, and others pathogenically. We observed that ABCs contribute to EAE in a protective manner, as knocking them out results in an exacerbation of disease, while in a model of SLE ABCs appear to be contributing pathogenically(12). We have previously found that knocking out ABCs has no impact on the clinical course of collagen-induced arthritis, though mice without ABCs do not show the γHV68-exacerbation of arthritis that is observed in control mice(45). The finding that ABCs are required for the γHV68 exacerbation of both CIA and EAE brings up the question of whether ABCs are a conserved mechanism by which gammaherpesvirus contributes to both arthritis and MS.

Critical to understanding this discrepancy in ABCs functioning protectively versus pathogenically in different models of autoimmunity is determining the mechanisms by which ABCs impact disease. Precisely how ABCs contribute to autoimmunity disease is unclear, and they may be contributing to different diseases through different mechanisms. It is intriguing that in a model of SLE, knocking out ABCs results in substantial changes to autoantibodies, yet we see no change in autoantibodies in models of EAE and CIA. Instead, we show here that during EAE and γHV68-EAE, knocking out ABCs results in altered peripheral T cell responses and lymphocyte infiltration of the CNS. In this context, ABCs may be functioning more as antigen-presenting cells rather than antibody-secreting cells. ABCs are known to be potent antigen

bioRxiv preprint doi: https://doi.org/10.1101/2021.07.22.453263; this version posted July 22, 2021. The copyright holder for this preprint (which was not certified by peer review) is the author/funder, who has granted bioRxiv a license to display the preprint in perpetuity. It is made available under aCC-BY 4.0 International license.

348 presenting cells and B cells contribute to EAE through their antigen presentation functions(46).

349 It remains unknown how ABCs are impacting disease in the CNS during γHV68-EAE, as
350 we do not observe differences in lymphocyte number or phenotype in KO mice. Other groups
351 have found that immune cell infiltration numbers and histopathological markers of CNS damage
352 do not reliably correlate with EAE severity(47,48). The increased γHV68 load in KO mice might
353 indicate viral reactivation. Our lab has previously shown that only latent γHV68, not lytic, leads
354 to exacerbation of EAE(38). Whether the virus is reactivating, and, if so, if the presence of the
355 lytic virus is modulating disease, deserves further examination.

356 In summary, we have shown that 1) EBV status and MS diagnosis impact the proportion of
357 circulating ABCs and their phenotype, 2) ABCs expand in the spleen in a sex-biased manner
358 during γHV68 infection and EAE, 3) ABCs display distinct phenotype during γHV68 infection and
359 EAE, and 4) knocking out ABCs results in exacerbation of EAE disease however loss of γHV68-
360 enhancement of EAE. We hope that these findings can contribute to better understanding of
361 the relationship between EBV and MS.

362 ## Methods

363 ### Donor recruitment and enrolment

364 Five individuals with relapsing MS were recruited at the Burnaby Hospital MS Clinic (Fraser
365 Health) under the supervision of Dr. Galina Vorobeychik. Seven unaffected donors were
366 recruited at the Life Sciences Center (University of British Columbia). All donors were female, 19
367 – 39 years of age (mean age 28 ± 6.4 years) and provided written informed consent prior to
368 enrolment in the study. Donors with a definite RRMS diagnosis, according to Poser or 2010
369 McDonald criteria, and disease duration of less than 10 years, were confirmed as treatment

bioRxiv preprint doi: https://doi.org/10.1101/2021.07.22.453263; this version posted July 22, 2021. The copyright holder for this preprint (which was not certified by peer review) is the author/funder, who has granted bioRxiv a license to display the preprint in perpetuity. It is made available under aCC-BY 4.0 International license.

naïve prior to donation (no previous use of any disease modifying therapies during lifetime). MS donors underwent a neurological exam the day of blood donation to assess Expanded Disability Status Scale (EDSS). Individuals with a progressive MS diagnosis or EDSS >4, that were male, pregnant, outside the designated age range, or undergoing treatment were excluded from the present study.

Donor blood collection and processing

Blood samples were obtained by venipuncture and assigned an alphanumeric identifier. Whole blood was processed for peripheral blood mononuclear cell (PBMC) isolation by Lymphoprep (StemCell) gradient separation, according to manufacturer's instructions, within an hour of collection in K2-EDTA coated vacutainer tubes (BD). Freshly isolated PBMC were counted and stained for flow cytometric analysis (no prior freezing or other preservation steps used). Serum was obtained by centrifugation of untreated blood samples and frozen at -80°C for subsequent analysis.

Donor serology

Antibodies to EBV and CMV were detected using enzyme-linked immunosorbent assays (ELISA) to determine donor history of infection. Nunc Maxisorp 96-well microtiter ELISA plates (Thermo Fisher Scientific) were coated overnight at 4°C with 1 µg/well of the peptide of interest in carbonate buffer. For EBV EBNA-1 and CMV, epitope peptides 1 and 2 were mixed together prior to well coating. The following day, the plates were washed with PBS and wash buffer (PBS + 0.05% Tween-20), followed by a two-hour blocking step at room temperature (RT) using wash buffer + 3% bovine serum albumin. Plates were washed again, then incubated with serum samples diluted in blocking buffer. Serum diluted 1:1000 was used to determine seropositivity

bioRxiv preprint doi: https://doi.org/10.1101/2021.07.22.453263; this version posted July 22, 2021. The copyright holder for this preprint (which was not certified by peer review) is the author/funder, who has granted bioRxiv a license to display the preprint in perpetuity. It is made available under aCC-BY 4.0 International license.

392 to EBV and CMV antigens. After a two-hour RT incubation with serum, the plates were washed,
393 then incubated with HRP-labelled goat anti-human IgG antibody (Thermo Fisher Scientific)
394 diluted 1:3000 in blocking buffer or HRP-labelled goat anti-human IgM (Thermo Fisher
395 Scientific) diluted 1:4000 at 37°C for 1 hour. The plates were then washed with PBS prior to the
396 addition of 100 µL/well TMB substrate (BD Biosciences). Fifteen minutes after the addition of
397 substrate, 100 µL stop solution (2 M sulfuric acid) was added to each well. The plates were read
398 at 450 nm on a VarioSkan Plate Reader (Thermo Fisher Scientific) within 10 minutes of adding
399 stop solution.

Antigen	**Peptide sequence**
EBV VCA p18	ASAGTGALASSAPSTAVAQSATPSVSSSISSLRAATSGATAAAAVDTGS GGGGQPHDTAPRGARKKQ
EBV EBNA-1	Epitope 1: RSPSSQSSSSGSPPRRPPPGRRPFFHPVG Epitope 2: DYFEYHQEGGPDGEPDVPPGAIEQGPADDPGEGPSTGPRG
CMV	Epitope 1: CETDDLDEEDTSIYLSPPPVPPVQVVAKRLPRPDTPRT Epitope 2: KSGTGPQPGSAGMGGAKTPSDAVQNILQKIEKIKNTEE

400

401 ## Mice

402 C57BL/6(J) mice were purchased from the Jackson Laboratory. *Tbx21*$^{fl/fl}$*Cd19*$^{cre/+}$ mice were
403 generated by crossing *Tbx21*$^{fl/fl}$*Cd19*$^{cre/+}$ and *Tbx21*$^{fl/fl}$*Cd19*$^{+/+}$ mice. *Tbx21*$^{fl/fl}$ and *Cd19*$^{cre/+}$ mice
404 were provided by Dr. Pippa Marrack(12). All animals were bred and maintained in the specific-
405 pathogen free animal facility at the University of British Columbia. All animal work was
406 performed in accordance with the regulation of the Canadian Council for Animal Care.

407 ## γHV68 infection

408 γHV68 (WUMS strain, purchased from ATCC) was propagated on Baby Hamster Kidney (BHK,
409 ATCC) cells and quantified by plaque assay. Mice were infected with γHV68 or mock-infected

bioRxiv preprint doi: https://doi.org/10.1101/2021.07.22.453263; this version posted July 22, 2021. The copyright holder for this preprint (which was not certified by peer review) is the author/funder, who has granted bioRxiv a license to display the preprint in perpetuity. It is made available under aCC-BY 4.0 International license.

with Minimum Essential Media (MEM, Gibco). For infection, virus was diluted in MEM and maintained sterile and on ice until infection. 6- to 10-week-old mice were infected intraperitoneally (i.p.) with 10^4 plaque-forming units (PFU) γHV68. No clinical symptoms were observed from viral infection.

Induction and evaluation of EAE

EAE was induced 35 days post- γHV68 infection by injecting 100 µl of emulsified Complete Freund's Adjuvant (DIFCO) containing 200 µg of MOG_{35-55} (GenScript) and 400 µg of desiccated Mycobacterium tuberculosis H37ra (DIFCO) subcutaneously. Mice also received two doses of 200 ng of pertussis toxin (List Biologicals) i.p. at the time of immunization and 48 hours post-induction. Mice were assessed daily (blinded) on a scale from 0 to 5: 0, no clinical symptoms, 0.5, partially limp tail; 1, paralyzed tail; 2, loss of coordination; 2.5, one hind limb paralyzed; 3, both hind limbs paralyzed; 3.5, both hind limbs paralyzed accompanied by weakness in the forelimbs; 4, forelimbs paralyzed (humane endpoint); 5, moribund or dead.

Tissue harvesting

Mice were euthanized by cardiac puncture while anesthetized with isoflurane and immediately perfused with 20cc PBS to allow for brain and spinal cord harvesting without blood contamination. Spleen, brain, and spinal cord were extracted, placed into PBS, and temporarily kept on ice until processing. Spleens and spinal cords were mashed through a 70 µm cell strainer and a single cell suspension prepared for each sample. Brains were mashed through a 70 µm cell strainer twice and a single-cell suspension was prepared for each sample. Splenocytes were incubated in Ammonium-Chloride-Potassium (ACK) lysing buffer for 10 minutes on ice to lyse red blood cells and remaining cells were kept on ice until further use.

bioRxiv preprint doi: https://doi.org/10.1101/2021.07.22.453263; this version posted July 22, 2021. The copyright holder for this preprint (which was not certified by peer review) is the author/funder, who has granted bioRxiv a license to display the preprint in perpetuity. It is made available under aCC-BY 4.0 International license.

Immune cells were isolated from brains and spinal cords using a 30% Percoll gradient (GE Healthcare) and were resuspended in Flow Cytometry Staining Buffer (FACS buffer, PBS with 2% newborn calf serum, Sigma-Aldrich) until staining.

Flow cytometric analysis of cell-type specific surface antigens and intracellular cytokines

To evaluate cytokine production by various cell types, 4 million splenocytes cells were stimulated ex vivo for 3 hours at 5% CO2 at 37°C in Minimum Essential Media (Gibco) containing 10% fetal bovine serum (FBS, Sigma-Aldrich), 1 μl/ml GolgiPlug (BD Biosciences), 10 ng/ml PMA (Sigma-Aldrich) and 500 ng/ml ionomycin (Thermo Fisher Scientific). Stimulated cells were then washed prior to staining. For each spleen sample, 4 million cells were stained in 2 wells of a 96-well plate, with 2 million cells per well. All collected brain and spinal cord cells were resuspended in FACS buffer and stained in a single well. Blood donor PBMC samples were stained at 1 million cells per well using the following method without ex vivo stimulation. Prior to staining, samples were incubated for 30 minutes at 4°C with 2 μl/ml Fixable Viability Dye eFluor506 (Thermo Fisher Scientific) while in PBS. Cells were then incubated with a rat anti-mouse CD16/32 (Fc block, BD Biosciences) antibody, or Human BD Fc Block (BD Biosciences) for PBMC samples, for 10 minutes at RT. Fluorochrome labeled antibodies against cell surface antigens were then added to the cells for 30 minutes covered from light at 4°C. After washing, cells were resuspended in Fix/Perm buffer (Thermo Fisher Scientific) for 30 minutes-12 hours covered from light minutes at 4°C, washed twice with Perm buffer, and incubated 40 minutes with antibodies against intracellular antigens in Perm buffer. Cells were then washed and resuspended in FACS buffer with 2 mM EDTA. Staining with antibodies from Thermo Fisher Scientific, Biolegend, and BD Biosciences. Samples collected on Attune NxT Flow Cytometer

bioRxiv preprint doi: https://doi.org/10.1101/2021.07.22.453263; this version posted July 22, 2021. The copyright holder for this preprint (which was not certified by peer review) is the author/funder, who has granted bioRxiv a license to display the preprint in perpetuity. It is made available under aCC-BY 4.0 International license.

454 (Thermo Fisher Scientific). Analyzed with FlowJo software version 10 (FlowJo LLC). Full-minus-

455 one controls used for gating.

Anti-human antibodies			
Antigen	**Fluorophore**	**Clone**	**Company**
CD19	APC-eFluor 780	HIB19	Thermo Fisher Scientific
IgD	FitC	IA6-2	BD Bioscience
CD11c	AlexaFluor 700	B-ly6	BD Bioscience
CD21	PerCpCy5.5	Bu32	Biolegend
CD20	Pacific Blue	2H7	Biolegend
CD27	Pe-Cy7	LG.3A1	Biolegend
Fas	PE Texas Red	DX2	BD Bioscience
PD1	PE	MIH4	Thermo Fisher Scientific

456

Anti-mouse antibodies			
Antigen	**Fluorophore**	**Clone**	**Company**
CD19	PE or FitC	ID3	Thermo Fisher Scientific
CD11c	APC	N418	Biolegend
CD11c	Alexafluor700	N418	Thermo Fisher Scientific
T-bet	PerCpCy5.5 or PE	4B10	Thermo Fisher Scientific
IgD	Pe-Cy7	11-26c	Thermo Fisher Scientific
IFNγ	APC	XMG1.2	Thermo Fisher Scientific
TNFα	Pe-Cy7	MP6-Xt22	Biolegend
IL-10	Pacific Blue	JES5-16E3	Biolegend
IL-17A	PE-Dazzle594	TCII-18H10.1	Biolegend
CTLA4	PE-Dazzle594	UC10-4B9	Biolegend
PDL1	SB436	MIH5	Thermo Fisher Scientific
PD1	SB436	J43	Thermo Fisher Scientific
IDO	PerCpeFluor 710	mIDO-48	Thermo Fisher Scientific
Fas	FitC	SA367H8	Biolegend
CD27	Pe-Cy7	LG.7F9	Biolegend
CD45	PerCpCy5.5	30-F11	Thermo Fisher Scientific
CD4	AlexaFluor 700	RM4-5	Thermo Fisher Scientific
CD8	APC-eFlour 780	53-6.7	Thermo Fisher Scientific
FoxP3	FitC	FJK-16S	Thermo Fisher Scientific
CD3e	eFluor 450	500A2	Thermo Fisher Scientific

457

bioRxiv preprint doi: https://doi.org/10.1101/2021.07.22.453263; this version posted July 22, 2021. The copyright holder for this preprint (which was not certified by peer review) is the author/funder, who has granted bioRxiv a license to display the preprint in perpetuity. It is made available under aCC-BY 4.0 International license.

Anti-MOG antibody ELISA

The sera were isolated by centrifugation 2000 × g for 10 min, aliquoted, and stored for up to 6 months at -80°C prior to running the ELISA. Anti-MOG_{35-55} antibodies were quantified by standard indirect ELISA. Briefly, ELISA plates (NUNC, Thermo Fisher Scientific) were coated with 1 µg MOG_{35-55} resuspended in coating buffer (0.05M carbonate buffer (pH 9.6)) overnight at 4°C. They were then washed 4x with wash buffer (PBS, 0.05% Tween-20), blocked with 5% newborn calf serum (NBCS, Sigma-Aldrich) for 1 hour at 37°C, incubated with serial dilutions (1:50 to 1:3200) of test sera diluted in blocking buffer for 2 hours at 37°C, and washed 4x wash buffer. Bound (anti-MOG_{35-55}) antibody was incubated with HRP-conjugated goat anti-mouse IgG2c (Thermo Fisher) diluted 1:500 in blocking buffer, for 1 hour at 37°C, washed 4x with wash buffer, and detected by TMB substrate addition (BD Biosciences). The plates were read at 450 nm on a VarioSkan Plate Reader (Thermo Fisher Scientific) within 10 minutes of adding stop solution.

γHV68 quantitation

Quantification of γHV68 load was done as previously described (49). gDNA was extracted from 4 x 10^6 splenocytes with PureLink Genomic DNA mini kit (Thermo Fisher Scientific), according to the manufacturer's instructions, and stored at -20°C. For quantitative qPCR, 150 ng DNA per reaction was amplified in duplicate using primers and probes specific to γHV68 *Orf50* and mouse *Ptger2* (see table) and 2× QuantiNova Probe Mastermix (Qiagen). Standard curves were obtained by serial dilutions of *Orf50* and *Ptger2* gBlocks (ORF50: $2x10^6$ – $2x10^1$; PTGER2: $5x10^7$-$5x10^2$). Run on the Bio-Rad CFX96 Touch™ Real Time PCR Detection system.

bioRxiv preprint doi: https://doi.org/10.1101/2021.07.22.453263; this version posted July 22, 2021. The copyright holder for this preprint (which was not certified by peer review) is the author/funder, who has granted bioRxiv a license to display the preprint in perpetuity. It is made available under aCC-BY 4.0 International license.

Gene	Sequence
Ptger2 Forward Primer	5'-TACCTTCAGCTGTACGCCAC-3'
Ptger2 Reverse Primer	5'-GCCAGGAGAATGAGGTGGTC-3'
Ptger2 Probe	5'-/56-FAM/CCTGCTGCT/ZEN/TATCGTGGCTG/3IABkFQ/-3'
Orf50 Forward Primer	5'-TGGACTTTGACAGCCCAGTA-3'
Orf50 Reverse Primer	5'- TCCCTTGAGGCAAATGATTC-3'
Orf50 Probe	5'-/56-FAM/TGACAGTGC/ZEN/CTATGGCCAAGTCTTG/3IABkFQ/-3'

Statistical analyses

Data and statistical analyses were performed using GraphPad Prism software 8.4.2 (GraphPad Software Inc.). Results are presented as mean ± SEM. Number of mice per group (n), statistical significance (p-value), and the number of experimental replicated as indicated in figure legend. Statistical analyses included: two-way ANOVA with Geisser-Greenhouse's correction, Mann-Whitney test, or one-way ANOVA. P-values indicated by asterisks as follows: ****p<0.0001, *** p<0.001, ** p<0.01, * p<0.05.

Study approval

Animal work was approved by the Animal Care Committee (ACC) of the University of British Columbia (Protocols A17- 0105, A17-0184). The human blood donation protocol (H16-02338) was approved by the University of British Columbia Clinical Research Ethics Board and by the Fraser Health Authority, General Neurology/Multiple Sclerosis.

Author contributions

ICM and MSH conceptualized project and designed experiments. ICM performed mouse experiments, analyzed data, and wrote the manuscript. JRA processed human donor samples and contributed to the manuscript. VF serotyped blood donors. AMG assisted with experiments

bioRxiv preprint doi: https://doi.org/10.1101/2021.07.22.453263; this version posted July 22, 2021. The copyright holder for this preprint (which was not certified by peer review) is the author/funder, who has granted bioRxiv a license to display the preprint in perpetuity. It is made available under aCC-BY 4.0 International license.

497 and developed MOG ELISA protocol. IS genotyped mice and assisted with experiments. GV

498 provided human donor samples.

499 Acknowledgements

500 We are grateful to Dr. Philippa Marrack for providing *Tbx21*$^{fl/fl}$ and *Cd19*$^{cre/+}$ mice. This research

501 was supported in part by the MSSC, CIHR, UBC, and JDRF. We express our gratitude to all the

502 blood donors who participated in this study.

bioRxiv preprint doi: https://doi.org/10.1101/2021.07.22.453263; this version posted July 22, 2021. The copyright holder for this preprint (which was not certified by peer review) is the author/funder, who has granted bioRxiv a license to display the preprint in perpetuity. It is made available under aCC-BY 4.0 International license.

503 Figures

bioRxiv preprint doi: https://doi.org/10.1101/2021.07.22.453263; this version posted July 22, 2021. The copyright holder for this preprint (which was not certified by peer review) is the author/funder, who has granted bioRxiv a license to display the preprint in perpetuity. It is made available under aCC-BY 4.0 International license.

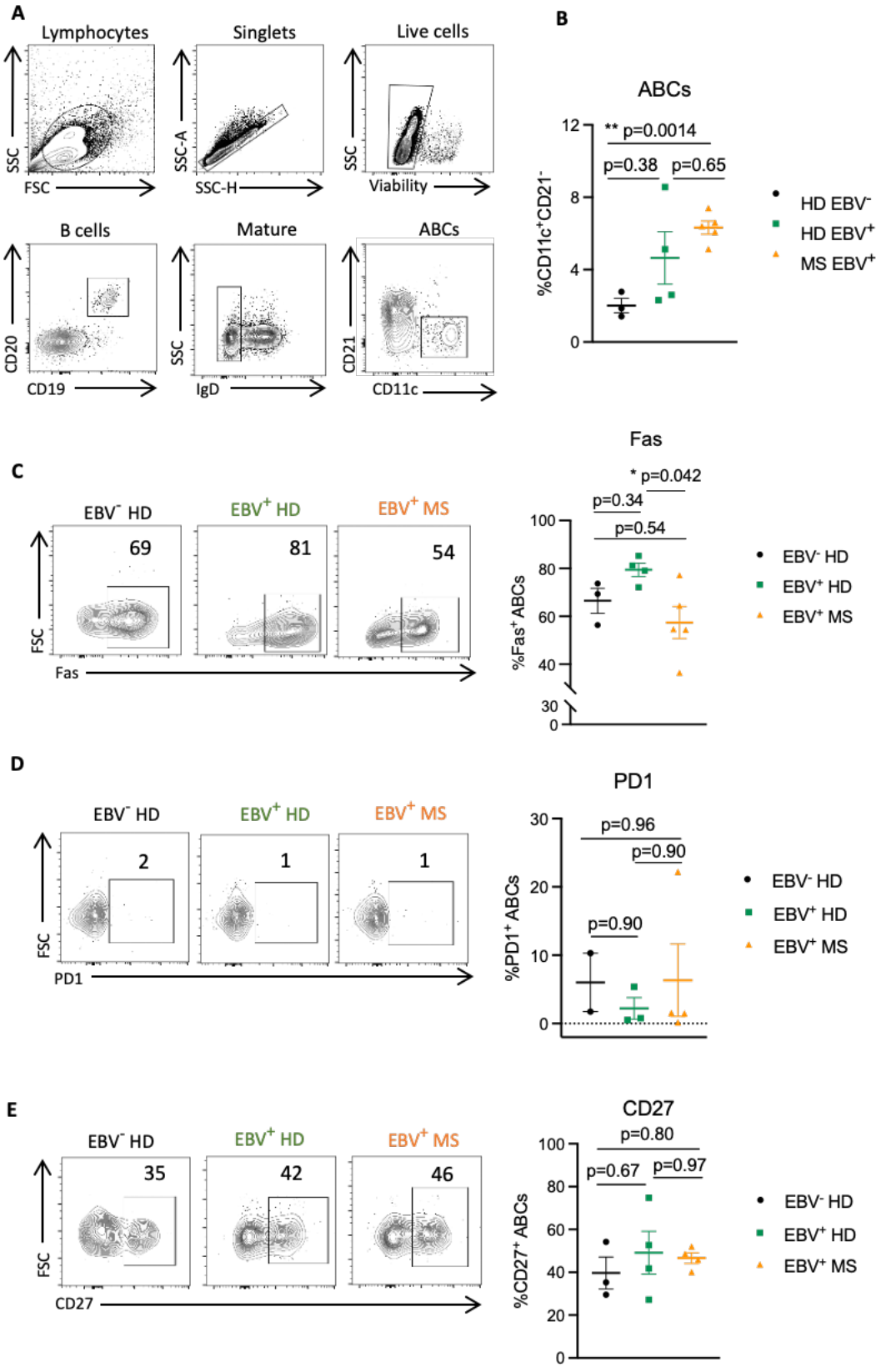

504

bioRxiv preprint doi: https://doi.org/10.1101/2021.07.22.453263; this version posted July 22, 2021. The copyright holder for this preprint (which was not certified by peer review) is the author/funder, who has granted bioRxiv a license to display the preprint in perpetuity. It is made available under aCC-BY 4.0 International license.

Figure 1: The peripheral ABC phenotype is impacted by EBV infection and MS status. PBMCs were collected from three EBV seronegative healthy females (EBV^- HD, black filled circles), four EBV seropositive healthy females (EBV^+ HD, green filled squares), and five females with relapse-remitting MS that are all EBV seropositive (EBV^+ MS, orange filled triangles). PBMCs were processed for flow cytometry immediately following isolation. (**A**) Representative gating strategy for ABCs ($CD19^+CD20^+CD11c^+CD21^-$) from PBMCs. (**B**) Proportion ABCs ($CD11c^+CD21^-$) among mature B cells ($CD19^+CD20^+IgD^-$). Representative samples and percent of ABCs ($CD19^+CD20^+CD11c^+CD21^-$) positive for (**C**) Fas (**D**) PD1, and (**E**) CD27. Data for CD27 and PD1 stained samples are fewer due to later addition of these markers following initial findings. Data presented as mean ± SEM, analyzed by one-way ANOVA with multiple comparisons, ** $p<0.01$, * $p<0.05$.

bioRxiv preprint doi: https://doi.org/10.1101/2021.07.22.453263; this version posted July 22, 2021. The copyright holder for this preprint (which was not certified by peer review) is the author/funder, who has granted bioRxiv a license to display the preprint in perpetuity. It is made available under aCC-BY 4.0 International license.

516

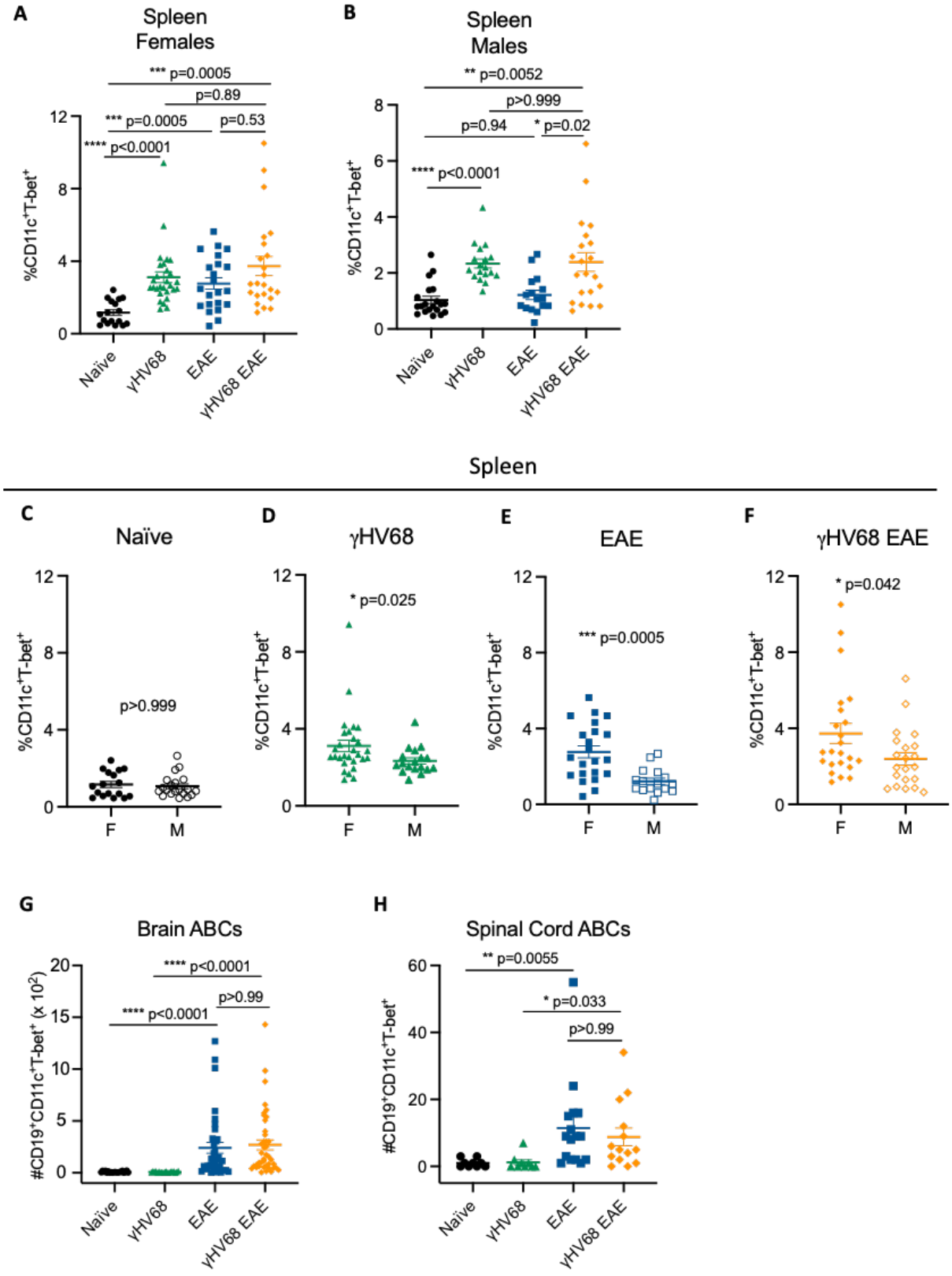

517

bioRxiv preprint doi: https://doi.org/10.1101/2021.07.22.453263; this version posted July 22, 2021. The copyright holder for this preprint (which was not certified by peer review) is the author/funder, who has granted bioRxiv a license to display the preprint in perpetuity. It is made available under aCC-BY 4.0 International license.

518 **Figure 2**: **ABCs are expanded in a sex-biased manner during γHV68 infection and EAE**.

519 C57BL/6(J) mice infected with γHV68 for 35 days to establish latency (γHV68, green triangles) or

520 mock-infected with blank medium (naïve, black circles). In some mice, MOG_{35-55} EAE was

521 induced 35 days after mock infection (EAE, blue squares) or initial infection (γHV68 EAE, orange

522 diamonds). At 35 days p.i. or 13 days post EAE induction, spleen, brain, and spinal cord

523 collected and processed for flow cytometry. (**A-B**) Proportion of ABCs ($CD11c^+T\text{-}bet^+$) of mature

524 B cells ($CD19^+IgD^-$) in the spleen of females and males. (**C-F**) Proportion of ABCs ($CD11c^+T\text{-}bet^+$)

525 of mature B cells ($CD19^+IgD^-$) in the spleen of females (F) and males (M). Data repeated from

526 panels A-B in panels C-F for better visualization and comparison of sex differences. (**G-H**)

527 Number of ABCs in the brain(**G**) and spinal cord(**H**). (**A-F**) Data pooled across 9 experiments,

528 n=16-29 per group. (**G-H**) Data pooled across 5 experiments, n=9-41 per group. Data presented

529 as mean ± SEM, analyzed by one-way ANOVA (**A, B**), Mann-Whitney (**C-F**), or Kruskal-Wallis (**G,**

530 **H**) test, ****p<0.0001, *** p<0.001; ** p<0.01, * p<0.05.

531

532

bioRxiv preprint doi: https://doi.org/10.1101/2021.07.22.453263; this version posted July 22, 2021. The copyright holder for this preprint (which was not certified by peer review) is the author/funder, who has granted bioRxiv a license to display the preprint in perpetuity. It is made available under aCC-BY 4.0 International license.

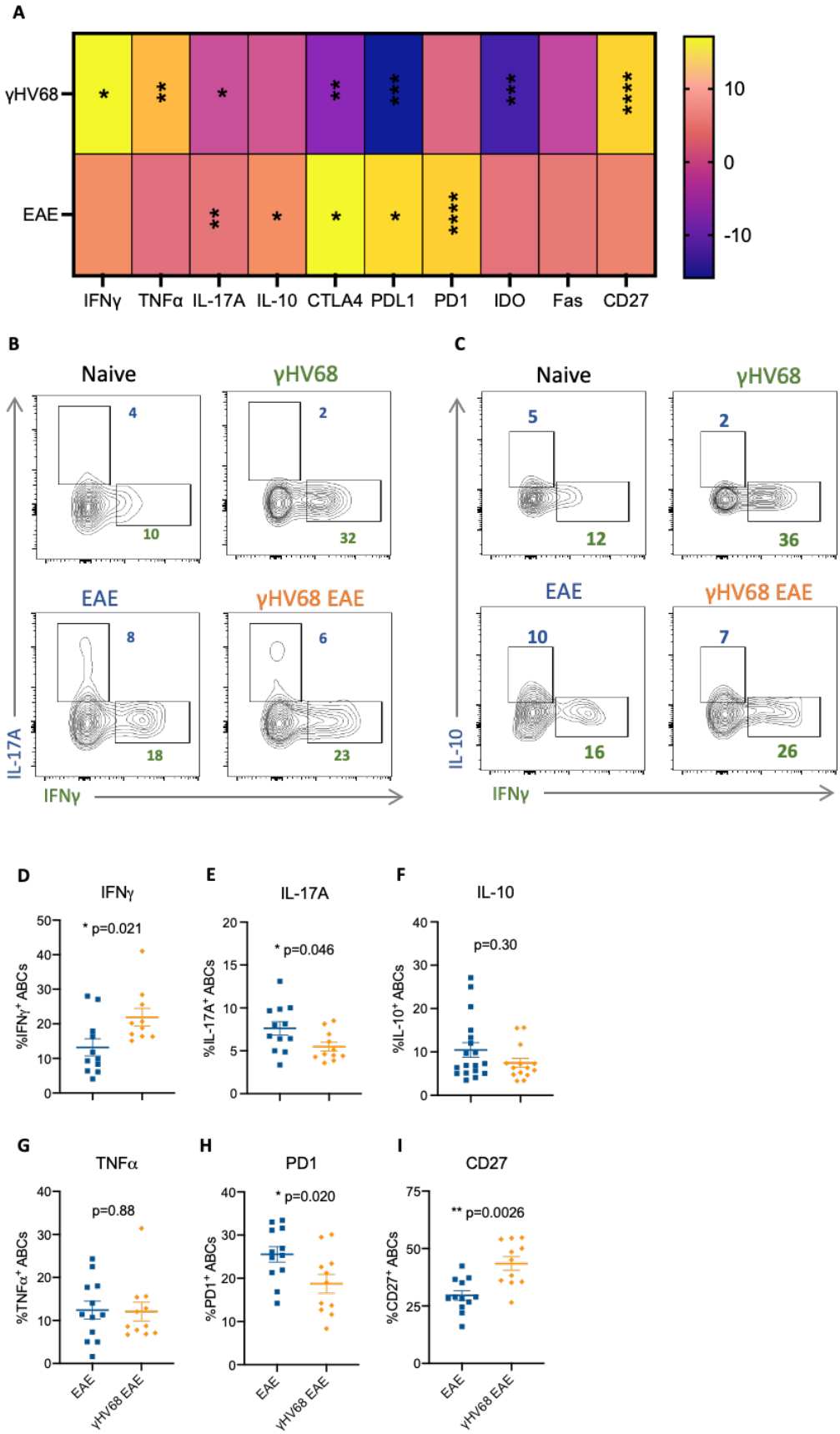

533

bioRxiv preprint doi: https://doi.org/10.1101/2021.07.22.453263; this version posted July 22, 2021. The copyright holder for this preprint (which was not certified by peer review) is the author/funder, who has granted bioRxiv a license to display the preprint in perpetuity. It is made available under aCC-BY 4.0 International license.

534 **Figure 3: γHV68 infection and EAE drive differential ABC phenotypes.** C57BL/6(J) mice infected
535 with γHV68 for 35 days (γHV68) or mock-infected (naïve). In some mice, MOG_{35-55} EAE was
536 induced 35 days after mock infection (EAE, blue squares) or initial infection (γHV68 EAE, orange
537 diamonds). At 35 days p.i. or 13 days post EAE induction, spleen collected and processed for
538 flow cytometry. (**A**) Heatmap – changes in frequency of ABC population expressing given
539 markers compared relative to naïve controls. (**B-C**) Representative flow plots. Previously gated
540 on $CD19^+CD11c^+T\text{-}bet^+$ ABCs in the spleen. Concatenated files. (**D-I**) Percent of splenic ABCs
541 ($CD19^+CD11c^+T\text{-}bet^+$) that are positive for (**D**) IFNγ, (**E**) IL-17A, (**F**) IL-10, (**G**) TNFα, (**H**) PD1, (**I**)
542 CD27. Data pooled across 2-3 experiments, n=9-18 per group. (**A**) Analyzed by one-way ANOVA
543 with multiple comparisons, compared to naïve, (**D-I**) data presented as mean ± SEM, analyzed
544 by Mann-Whitney test, ****p<0.0001, *** p<0.001, ** p<0.01, * p<0.05.
545

bioRxiv preprint doi: https://doi.org/10.1101/2021.07.22.453263; this version posted July 22, 2021. The copyright holder for this preprint (which was not certified by peer review) is the author/funder, who has granted bioRxiv a license to display the preprint in perpetuity. It is made available under aCC-BY 4.0 International license.

546

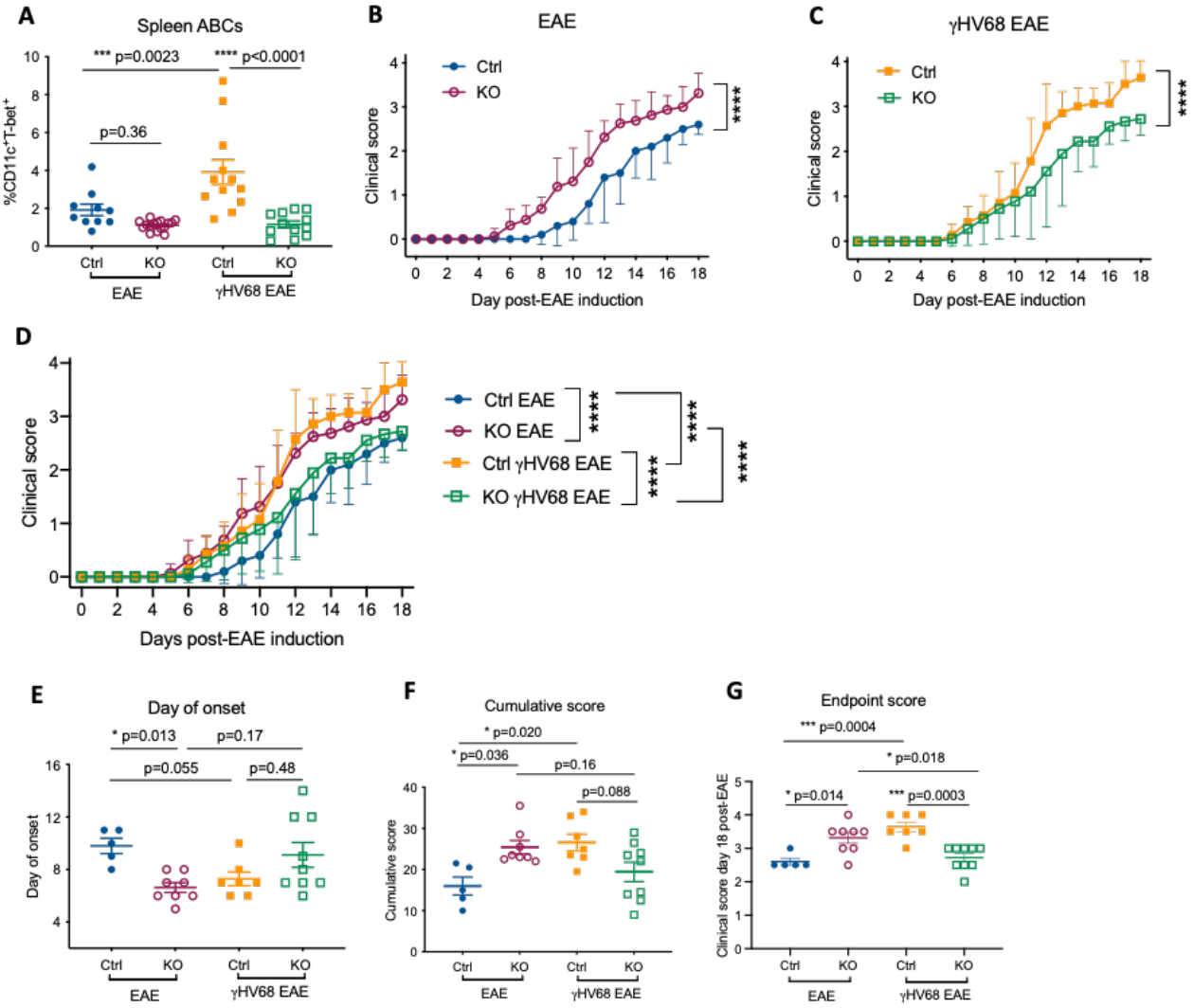

547

548

549 **Figure 4: EAE disease course is altered in ABC KO mice.** Female *Tbx21*$^{fl/fl}$*Cd19*$^{cre/+}$ (KO) and

550 *Tbx21*$^{fl/fl}$*Cd19*$^{+/+}$ (Ctrl) mice were infected with γHV68 or mock-infected for 35 days and then

551 induced for MOG_{35-55} EAE and clinically monitored for 18 days. (**A**) Percent ABCs ($CD11c^+T\text{-}bet^+$)

552 of mature B cells ($CD19^+IgD^-$) in the spleen. (**B-D**) EAE clinical scores. Data in panel D is repeated

553 from panels B-C. Data are pooled across three experiments, n=5-9 per group, representative of

554 five independent experiments. (**E**) Day of clinical symptom onset. (**F**) Cumulative score (**G**)

bioRxiv preprint doi: https://doi.org/10.1101/2021.07.22.453263; this version posted July 22, 2021. The copyright holder for this preprint (which was not certified by peer review) is the author/funder, who has granted bioRxiv a license to display the preprint in perpetuity. It is made available under aCC-BY 4.0 International license.

555 endpoint score at day 18 post-EAE induction. Data analyzed by (**A, E-G**) one-way ANOVA, (**B-C**)

556 two-way ANOVA, (**D**) two-way ANOVA with multiple comparisons. Data presented as mean ±

557 SEM (**A, E-G**) or mean ± SD (**B-D**), ****p<0.0001, *** p<0.001, ** p<0.01, * p<0.05.

558

559

bioRxiv preprint doi: https://doi.org/10.1101/2021.07.22.453263; this version posted July 22, 2021. The copyright holder for this preprint (which was not certified by peer review) is the author/funder, who has granted bioRxiv a license to display the preprint in perpetuity. It is made available under aCC-BY 4.0 International license.

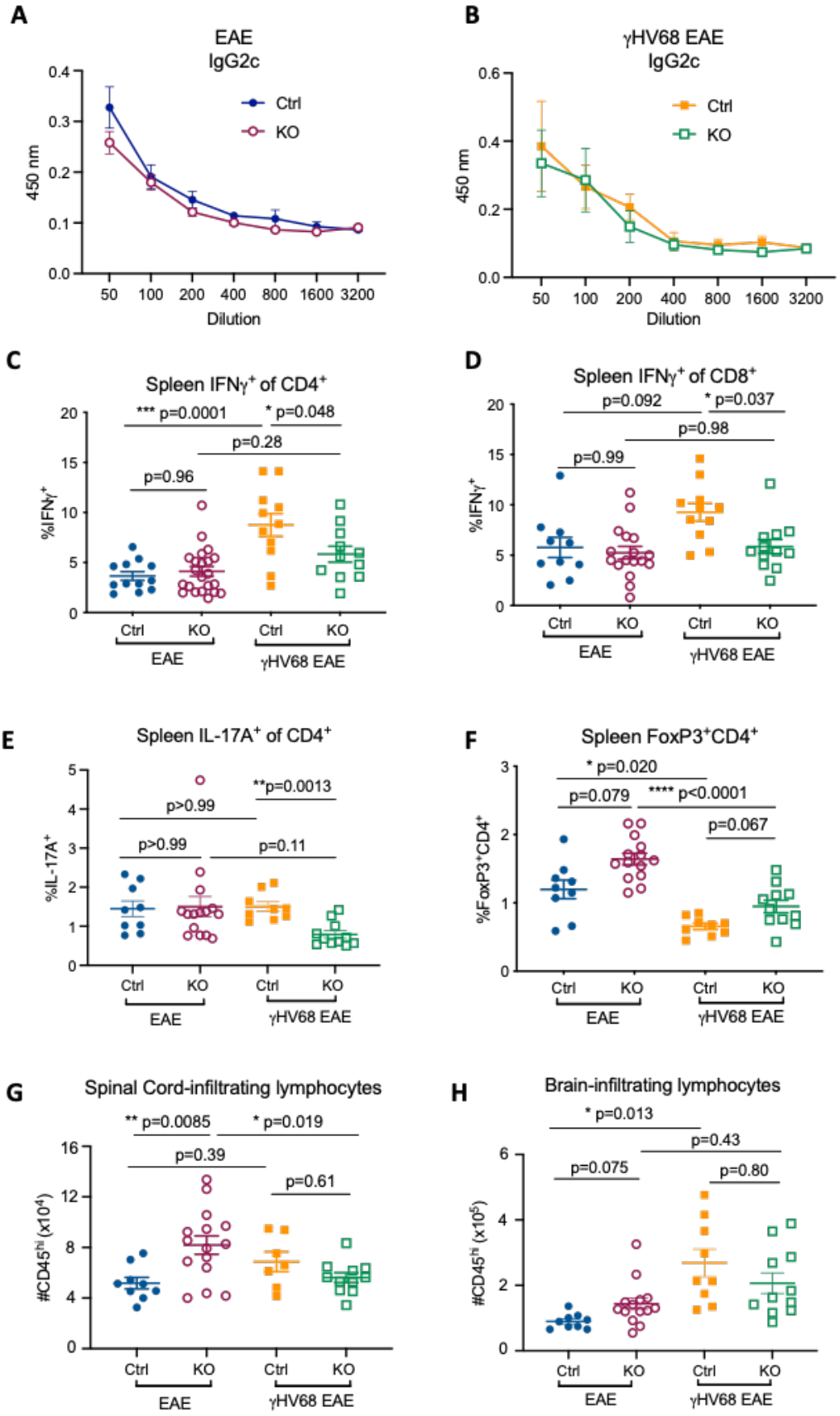

560

bioRxiv preprint doi: https://doi.org/10.1101/2021.07.22.453263; this version posted July 22, 2021. The copyright holder for this preprint (which was not certified by peer review) is the author/funder, who has granted bioRxiv a license to display the preprint in perpetuity. It is made available under aCC-BY 4.0 International license.

Figure 5: Immune profile, but not autoantibodies, is altered in ABC KO mice. Female *Tbx21*$^{fl/fl}$*Cd19*$^{cre/+}$ (KO) and *Tbx21*$^{fl/fl}$*Cd19*$^{+/+}$ (Ctrl) mice were infected with γHV68 or mock-infected for 35 days and then induced for MOG_{35-55} EAE. At day 13-18 post-EAE induction blood (serum), spleen, brain, and spinal cord collected. Spleen, brain, and spinal cord processed for flow cytometry. (**A-B**) Optical density (O.D., y-axis) reflecting titers (x-axis; dilution of serum) of IgG2c anti-MOG_{35-55} antibodies in Ctrl and KO mice, separated by EAE (**A**) and γHV68 EAE (**B**) mice, n=3-6 mice per group. (**C-D**) Percent IFNγ$^+$ of CD3$^+$CD4$^+$ (**C**) and CD3$^+$CD8$^+$ (**D**) cells in the spleen. (**E**) Percent of CD3$^+$CD4$^+$ cells in the spleen expressing IL-17A. (**F**) Percent of live cells in the spleen that are CD4$^+$FoxP3$^+$. (**G-H**) Number of CD45^{hi} cells in the spinal cord (**G**) and brain (**H**). Data presented as mean ± SEM. (**C-H**) Analyzed by one way ANOVA with multiple comparisons, ****p<0.0001, *** p<0.001, ** p<0.01, * p<0.05.

bioRxiv preprint doi: https://doi.org/10.1101/2021.07.22.453263; this version posted July 22, 2021. The copyright holder for this preprint (which was not certified by peer review) is the author/funder, who has granted bioRxiv a license to display the preprint in perpetuity. It is made available under aCC-BY 4.0 International license.

References

1. Hao Y, O'Neill P, Naradikian MS, Scholz JL, Cancro MP. A B-cell subset uniquely responsive to innate stimuli accumulates in aged mice. Blood. 2011 Aug 4;118(5):1294–304.

2. Rubtsova K, Rubtsov AV, van Dyk LF, Kappler JW, Marrack P. T-box transcription factor T-bet, a key player in a unique type of B-cell activation essential for effective viral clearance. Proc Natl Acad Sci U S A. 2013 Aug 20;110(34):E3216-3224.

3. Rubtsov AV, Rubtsova K, Fischer A, Meehan RT, Gillis JZ, Kappler JW, et al. Toll-like receptor 7 (TLR7)-driven accumulation of a novel CD11c^{+} B-cell population is important for the development of autoimmunity. Blood. 2011 Aug 4;118(5):1305–15.

4. Ratliff M, Alter S, Frasca D, Blomberg BB, Riley RL. In senescence, age-associated B cells secrete TNFα and inhibit survival of B-cell precursors*. Aging Cell. 2013 Apr 1;12(2):303–11.

5. Rubtsov AV, Rubtsova K, Kappler JW, Jacobelli J, Friedman RS, Marrack P. CD11c-expressing B cells are located at the T cell B cell border in spleen and are potent antigen presenting cells. J Immunol Baltim Md 1950. 2015 Jul 1;195(1):71–9.

6. Claes N, Fraussen J, Vanheusden M, Hellings N, Stinissen P, Van Wijmeersch B, et al. Age-Associated B Cells with Proinflammatory Characteristics Are Expanded in a Proportion of Multiple Sclerosis Patients. J Immunol Baltim Md 1950. 2016 15;197(12):4576–83.

7. Isnardi I, Ng Y-S, Menard L, Meyers G, Saadoun D, Srdanovic I, et al. Complement receptor 2/CD21- human naive B cells contain mostly autoreactive unresponsive clones. Blood. 2010 Jun 17;115(24):5026–36.

8. Wehr C, Eibel H, Masilamani M, Illges H, Schlesier M, Peter H-H, et al. A new CD21low B cell population in the peripheral blood of patients with SLE. Clin Immunol Orlando Fla. 2004 Nov;113(2):161–71.

9. Rakhmanov M, Keller B, Gutenberger S, Foerster C, Hoenig M, Driessen G, et al. Circulating CD21low B cells in common variable immunodeficiency resemble tissue homing, innate-like B cells. Proc Natl Acad Sci U S A. 2009 Aug 11;106(32):13451–6.

10. Wang S, Wang J, Kumar V, Karnell JL, Naiman B, Gross PS, et al. IL-21 drives expansion and plasma cell differentiation of autoreactive CD11c hi T-bet + B cells in SLE. Nat Commun [Internet]. 2018 May 1 [cited 2018 Nov 2];9(1):1758. Available from: https://www.nature.com/articles/s41467-018-03750-7

11. Thorarinsdottir K, Camponeschi A, Jonsson C, Granhagen Önnheim K, Nilsson J, Forslind K, et al. CD21-/low B cells associate with joint damage in rheumatoid arthritis patients. Scand J Immunol. 2019 Aug;90(2):e12792.

bioRxiv preprint doi: https://doi.org/10.1101/2021.07.22.453263; this version posted July 22, 2021. The copyright holder for this preprint (which was not certified by peer review) is the author/funder, who has granted bioRxiv a license to display the preprint in perpetuity. It is made available under aCC-BY 4.0 International license.

12. Rubtsova K, Rubtsov AV, Thurman JM, Mennona JM, Kappler JW, Marrack P. B cells expressing the transcription factor T-bet drive lupus-like autoimmunity. J Clin Invest. 2017 May 12;127(4):1392–404.

13. Rubtsova K, Rubtsov AV, Cancro MP, Marrack P. Age-associated B cells: A T-bet dependent effector with roles in protective and pathogenic immunity. J Immunol Baltim Md 1950 [Internet]. 2015 Sep 1 [cited 2018 Nov 5];195(5):1933–7. Available from: https://www.ncbi.nlm.nih.gov/pmc/articles/PMC4548292/

14. Nath N, Prasad R, Giri S, Singh AK, Singh I. T-bet is essential for the progression of experimental autoimmune encephalomyelitis. Immunology. 2006 Jul;118(3):384–91.

15. Rubtsova K, Rubtsov AV, Halemano K, Li SX, Kappler JW, Santiago ML, et al. T Cell Production of IFNγ in Response to TLR7/IL-12 Stimulates Optimal B Cell Responses to Viruses. PloS One. 2016;11(11):e0166322.

16. Knox JJ, Buggert M, Kardava L, Seaton KE, Eller MA, Canaday DH, et al. T-bet+ B cells are induced by human viral infections and dominate the HIV gp140 response. JCI Insight. 2017 Apr 20;2(8).

17. Johnson JL, Rosenthal RL, Knox JJ, Myles A, Naradikian MS, Madej J, et al. The Transcription Factor T-bet Resolves Memory B Cell Subsets with Distinct Tissue Distributions and Antibody Specificities in Mice and Humans. Immunity [Internet]. 2020 Apr 29 [cited 2020 May 15]; Available from: http://www.sciencedirect.com/science/article/pii/S1074761320301333

18. Rubtsova K, Rubtsov AV, Dyk LF van, Kappler JW, Marrack P. T-box transcription factor T-bet, a key player in a unique type of B-cell activation essential for effective viral clearance. Proc Natl Acad Sci [Internet]. 2013 Aug 20 [cited 2018 Nov 2];110(34):E3216–24. Available from: http://www.pnas.org/content/110/34/E3216

19. A N, E Z, Cd S, Rg K, Cm T, Cf F, et al. Influenza-specific effector memory B cells predict long-lived antibody responses to vaccination in humans. 2019 May 20 [cited 2021 Jun 1]; Available from: https://europepmc.org/article/ppr/ppr79744

20. Austin JW, Buckner CM, Kardava L, Wang W, Zhang X, Melson VA, et al. Overexpression of T-bet in HIV infection is associated with accumulation of B cells outside germinal centers and poor affinity maturation. Sci Transl Med [Internet]. 2019 Nov 27 [cited 2021 Jun 1];11(520). Available from: https://stm.sciencemag.org/content/11/520/eaax0904

21. Chang L-Y, Li Y, Kaplan DE. Hepatitis C viraemia reversibly maintains subset of antigen-specific T-bet+ tissue-like memory B cells. J Viral Hepat [Internet]. 2017 May [cited 2020 May 15];24(5):389–96. Available from: https://www.ncbi.nlm.nih.gov/pmc/articles/PMC5637374/

bioRxiv preprint doi: https://doi.org/10.1101/2021.07.22.453263; this version posted July 22, 2021. The copyright holder for this preprint (which was not certified by peer review) is the author/funder, who has granted bioRxiv a license to display the preprint in perpetuity. It is made available under aCC-BY 4.0 International license.

641 22. Eccles JD, Turner RB, Kirk NA, Muehling LM, Borish L, Steinke JW, et al. T-bet+ Memory B
642 Cells Link to Local Cross-Reactive IgG upon Human Rhinovirus Infection. Cell Rep
643 [Internet]. 2020 Jan 14 [cited 2021 Jun 1];30(2):351-366.e7. Available from:
644 https://www.sciencedirect.com/science/article/pii/S2211124719316778

645 23. Holla P, Dizon B, Ambegaonkar AA, Rogel N, Goldschmidt E, Boddapati AK, et al. Shared
646 transcriptional profiles of atypical B cells suggest common drivers of expansion and
647 function in malaria, HIV, and autoimmunity. Sci Adv [Internet]. 2021 May 26 [cited 2021
648 Jun 24];7(22):eabg8384. Available from:
649 https://www.ncbi.nlm.nih.gov/pmc/articles/PMC8153733/

650 24. Cohen JI. Epstein–Barr Virus Infection. N Engl J Med. 2000 Aug 17;343(7):481–92.

651 25. Fraser KB, Millar JHD, Haire M, Mccrea S. INCREASED TENDENCY TO SPONTANEOUS IN-
652 VITRO LYMPHOCYTE TRANSFORMATION IN CLINICALLY ACTIVE MULTIPLE SCLEROSIS. The
653 Lancet. 1979 Oct 6;314(8145):715–7.

654 26. Ascherio A, Munger KL, Lennette ET, Spiegelman D, Hernán MA, Olek MJ, et al. Epstein-Barr
655 virus antibodies and risk of multiple sclerosis: a prospective study. JAMA. 2001 Dec
656 26;286(24):3083–8.

657 27. Farrell RA, Antony D, Wall GR, Clark DA, Fisniku L, Swanton J, et al. Humoral immune
658 response to EBV in multiple sclerosis is associated with disease activity on MRI. Neurology
659 [Internet]. 2009 Jul 7 [cited 2019 Mar 22];73(1):32–8. Available from:
660 https://www.ncbi.nlm.nih.gov/pmc/articles/PMC2848585/

661 28. Pender MP, Csurhes PA, Burrows JM, Burrows SR. Defective T-cell control of Epstein–Barr
662 virus infection in multiple sclerosis. Clin Transl Immunol [Internet]. 2017 Jan 20 [cited 2019
663 Mar 22];6(1):e126. Available from:
664 https://www.ncbi.nlm.nih.gov/pmc/articles/PMC5292561/

665 29. James JA, Kaufman KM, Farris AD, Taylor-Albert E, Lehman TJ, Harley JB. An increased
666 prevalence of Epstein-Barr virus infection in young patients suggests a possible etiology for
667 systemic lupus erythematosus. J Clin Invest [Internet]. 1997 Dec 15 [cited 2021 Jun
668 1];100(12):3019–26. Available from:
669 https://www.ncbi.nlm.nih.gov/pmc/articles/PMC508514/

670 30. James JA, Neas BR, Moser KL, Hall T, Bruner GR, Sestak AL, et al. Systemic lupus
671 erythematosus in adults is associated with previous Epstein-Barr virus exposure. Arthritis
672 Rheum. 2001 May;44(5):1122–6.

673 31. Li Z-X, Zeng S, Wu H-X, Zhou Y. The risk of systemic lupus erythematosus associated with
674 Epstein-Barr virus infection: a systematic review and meta-analysis. Clin Exp Med. 2019
675 Feb;19(1):23–36.

bioRxiv preprint doi: https://doi.org/10.1101/2021.07.22.453263; this version posted July 22, 2021. The copyright holder for this preprint (which was not certified by peer review) is the author/funder, who has granted bioRxiv a license to display the preprint in perpetuity. It is made available under aCC-BY 4.0 International license.

676 32. Balandraud N, Meynard JB, Auger I, Sovran H, Mugnier B, Reviron D, et al. Epstein-Barr virus
677 load in the peripheral blood of patients with rheumatoid arthritis: accurate quantification
678 using real-time polymerase chain reaction. Arthritis Rheum. 2003 May;48(5):1223–8.

679 33. Ferrell PB, Aitcheson CT, Pearson GR, Tan EM. Seroepidemiological study of relationships
680 between Epstein-Barr virus and rheumatoid arthritis. J Clin Invest. 1981 Mar;67(3):681–7.

681 34. Alspaugh MA, Henle G, Lennette ET, Henle W. Elevated levels of antibodies to Epstein-Barr
682 virus antigens in sera and synovial fluids of patients with rheumatoid arthritis. J Clin Invest.
683 1981 Apr;67(4):1134–40.

684 35. Márquez AC, Horwitz MS. The Role of Latently Infected B Cells in CNS Autoimmunity. Front
685 Immunol [Internet]. 2015 Oct 28 [cited 2017 Apr 5];6. Available from:
686 http://www.ncbi.nlm.nih.gov/pmc/articles/PMC4623415/

687 36. Bar-Or A, Pender MP, Khanna R, Steinman L, Hartung H-P, Maniar T, et al. Epstein-Barr Virus
688 in Multiple Sclerosis: Theory and Emerging Immunotherapies. Trends Mol Med. 2020
689 Mar;26(3):296–310.

690 37. Olivadoti M, Toth LA, Weinberg J, Opp MR. Murine gammaherpesvirus 68: a model for the
691 study of Epstein-Barr virus infections and related diseases. Comp Med. 2007 Feb;57(1):44–
692 50.

693 38. Casiraghi C, Shanina I, Cho S, Freeman ML, Blackman MA, Horwitz MS. Gammaherpesvirus
694 Latency Accentuates EAE Pathogenesis: Relevance to Epstein-Barr Virus and Multiple
695 Sclerosis. PLOS Pathog [Internet]. 2012 May 17 [cited 2018 Dec 13];8(5):e1002715.
696 Available from:
697 https://journals.plos.org/plospathogens/article?id=10.1371/journal.ppat.1002715

698 39. Casiraghi C, Márquez AC, Shanina I, Horwitz MS. Latent virus infection upregulates CD40
699 expression facilitating enhanced autoimmunity in a model of multiple sclerosis. Sci Rep.
700 2015 Sep 10;5:srep13995.

701 40. Lau D, Lan LY-L, Andrews SF, Henry C, Rojas KT, Neu KE, et al. Low CD21 expression defines
702 a population of recent germinal center graduates primed for plasma cell differentiation.
703 Sci Immunol. 2017 Jan 27;2(7).

704 41. Barnett BE, Staupe RP, Odorizzi PM, Palko O, Tomov VT, Mahan AE, et al. B cell intrinsic T-
705 bet expression is required to control chronic viral infection. J Immunol Baltim Md 1950
706 [Internet]. 2016 Aug 15 [cited 2018 Nov 13];197(4):1017–22. Available from:
707 https://www.ncbi.nlm.nih.gov/pmc/articles/PMC4975981/

708 42. Rubtsova K, Marrack P, Rubtsov AV. Age-associated B cells: are they the key to
709 understanding why autoimmune diseases are more prevalent in women? Expert Rev Clin
710 Immunol [Internet]. 2012 Jan [cited 2021 Jun 1];8(1):5–7. Available from:
711 https://www.ncbi.nlm.nih.gov/pmc/articles/PMC3940262/

bioRxiv preprint doi: https://doi.org/10.1101/2021.07.22.453263; this version posted July 22, 2021. The copyright holder for this preprint (which was not certified by peer review) is the author/funder, who has granted bioRxiv a license to display the preprint in perpetuity. It is made available under aCC-BY 4.0 International license.

712 43. Palaszynski KM, Loo KK, Ashouri JF, Liu H, Voskuhl RR. Androgens are protective in
713 experimental autoimmune encephalomyelitis: implications for multiple sclerosis. J
714 Neuroimmunol. 2004 Jan;146(1–2):144–52.

715 44. Okuda Y, Okuda M, Bernard CCA. Gender does not influence the susceptibility of C57BL/6
716 mice to develop chronic experimental autoimmune encephalomyelitis induced by myelin
717 oligodendrocyte glycoprotein. Immunol Lett. 2002 Apr 1;81(1):25–9.

718 45. Mouat IC, Morse ZJ, Shanina I, Brown KL, Horwitz MS. Latent gammaherpesvirus
719 exacerbates arthritis through modification of age-associated B cells. Valenzano DR, editor.
720 eLife [Internet]. 2021 Jun 3 [cited 2021 Jun 6];10:e67024. Available from:
721 https://doi.org/10.7554/eLife.67024

722 46. Molnarfi N, Schulze-Topphoff U, Weber MS, Patarroyo JC, Prod'homme T, Varrin-Doyer M,
723 et al. MHC class II-dependent B cell APC function is required for induction of CNS
724 autoimmunity independent of myelin-specific antibodies. J Exp Med. 2013 Dec
725 16;210(13):2921–37.

726 47. Goncalves DaSilva A, Liaw L, Yong VW. Cleavage of Osteopontin by Matrix
727 Metalloproteinase-12 Modulates Experimental Autoimmune Encephalomyelitis Disease in
728 C57BL/6 Mice. Am J Pathol [Internet]. 2010 Sep [cited 2021 Jun 2];177(3):1448–58.
729 Available from: https://www.ncbi.nlm.nih.gov/pmc/articles/PMC2928976/

730 48. Doss PMIA, Umair M, Baillargeon J, Fazazi R, Fudge N, Akbar I, et al. Male sex chromosomal
731 complement exacerbates the pathogenicity of Th17 cells in a chronic model of central
732 nervous system autoimmunity. Cell Rep. 2021 Mar 9;34(10):108833.

733 49. Márquez AC, Shanina I, Horwitz MS. Multiple Sclerosis-Like Symptoms in Mice Are Driven by
734 Latent γHerpesvirus-68 Infected B Cells. Front Immunol [Internet]. 2020 [cited 2021 Apr
735 12];11. Available from:
736 https://www.frontiersin.org/articles/10.3389/fimmu.2020.584297/full

737

738

bioRxiv preprint doi: https://doi.org/10.1101/2021.07.22.453263; this version posted July 22, 2021. The copyright holder for this preprint (which was not certified by peer review) is the author/funder, who has granted bioRxiv a license to display the preprint in perpetuity. It is made available under aCC-BY 4.0 International license.

Supplement

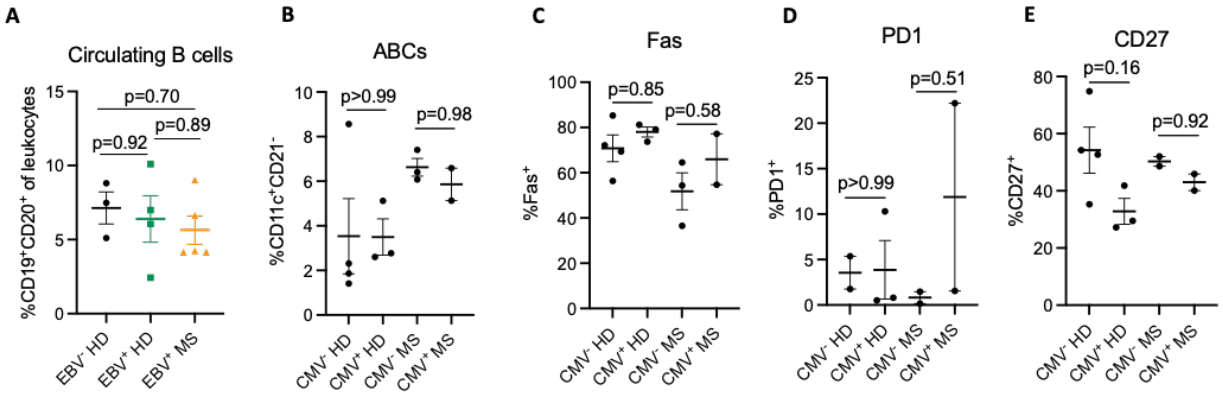

Supplemental Figure 1: ABC phenotype is not impacted by CMV status. Same donors as Figure 1, here classified by CMV, rather than EBV status. PBMCs were collected from four CMV seronegative healthy females (CMV^- HD), three CMV seropositive healthy females (CMV^+ HD), three CMV seronegative females with relapse-remitting MS (CMV^- MS), and two CMV seropositive females with relapse-remitting MS (CMV^+ MS). PBMCs were processed for flow cytometry immediately following isolation. (**A**) Proportion of B cells ($CD19^+CD20^+$) of leukocytes, separated by EBV and MS status. (**B**) Proportion ABCs ($CD11c^+CD21^-$) among mature B cells ($CD19^+CD20^+IgD^-$), separated by CMV status. (**C-E**) Percent of ABCs ($CD19^+$ $CD20^+CD11c^+CD21^-$) positive for (**C**) Fas, (**D**) PD1, and (**E**) CD27. Data presented as mean ± SEM, analyzed by one-way ANOVA with multiple comparisons.

bioRxiv preprint doi: https://doi.org/10.1101/2021.07.22.453263; this version posted July 22, 2021. The copyright holder for this preprint (which was not certified by peer review) is the author/funder, who has granted bioRxiv a license to display the preprint in perpetuity. It is made available under aCC-BY 4.0 International license.

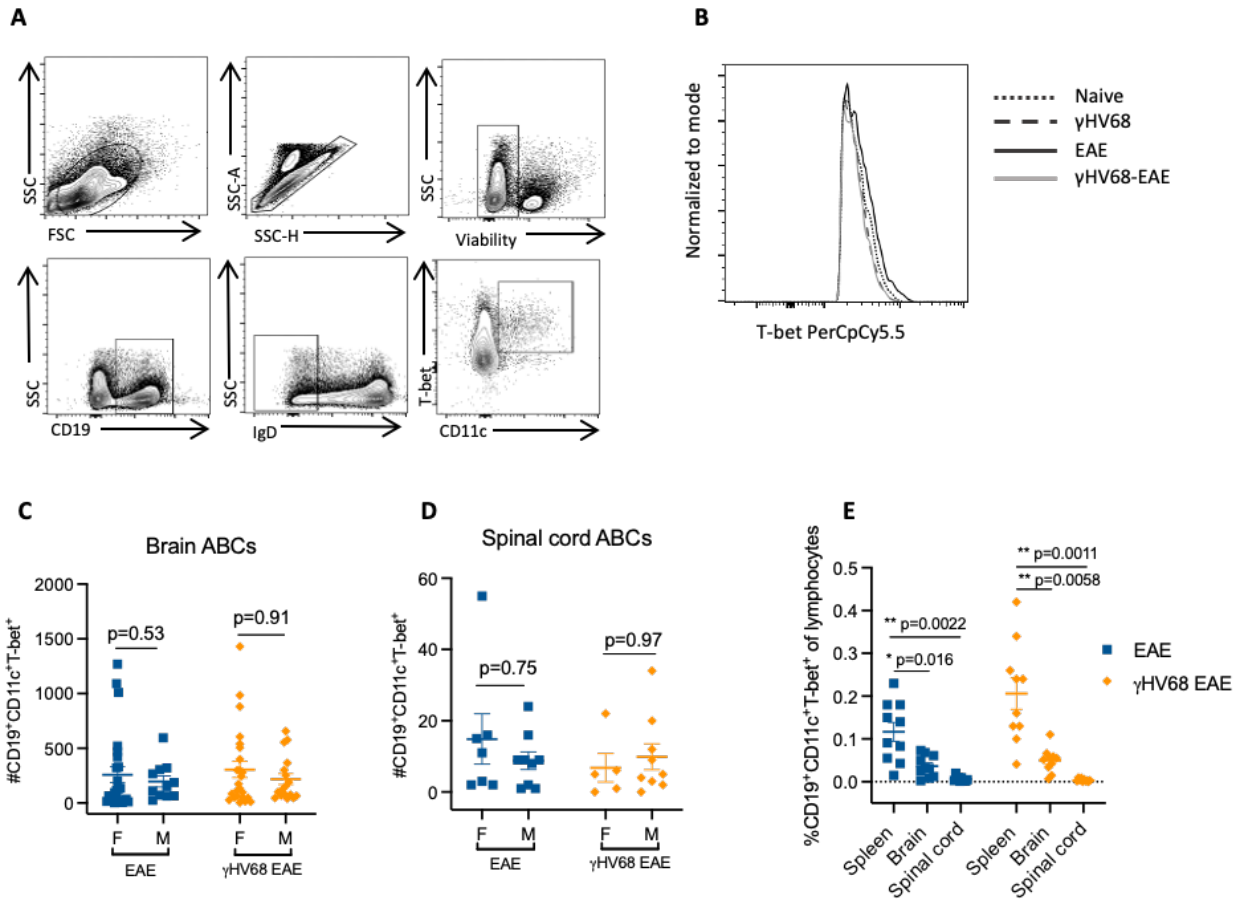

Supplemental Figure 2: (**A**) Representative gating of ABCs: lymphocytes, singlets, live cells, $CD19^+$ B cells, IgD^- mature B cells, $CD11c^+T\text{-}bet^+$ ABCs. (**B**) Representative expression of T-bet on ABCs ($CD19^+CD11c^+T\text{-}bet^+$) in the spleen from naïve, latently γHV68-infected (35 days p.i.), EAE (13-15 days post-induction), and γHV68-EAE (13-15 days post-induction). (**C-D**) Number of ABCs ($CD19^+CD11c^+T\text{-}bet^+$) in the brain (**C**) or spinal cord (**D**) of mice induced for EAE (13-15 days post-induction) and γHV68-EAE (13-15 days post-induction), as determined by flow cytometry. (**C-D**) Data pooled across 5 experiments, n=5-25 per group. (**E**) Percent of ABCs of live leukocytes in the spleen, brain, and spinal cord. Data presented as mean ± SEM, analyzed by one-way ANOVA test, *** p<0.001; ** p<0.01, * p<0.05.

bioRxiv preprint doi: https://doi.org/10.1101/2021.07.22.453263; this version posted July 22, 2021. The copyright holder for this preprint (which was not certified by peer review) is the author/funder, who has granted bioRxiv a license to display the preprint in perpetuity. It is made available under aCC-BY 4.0 International license.

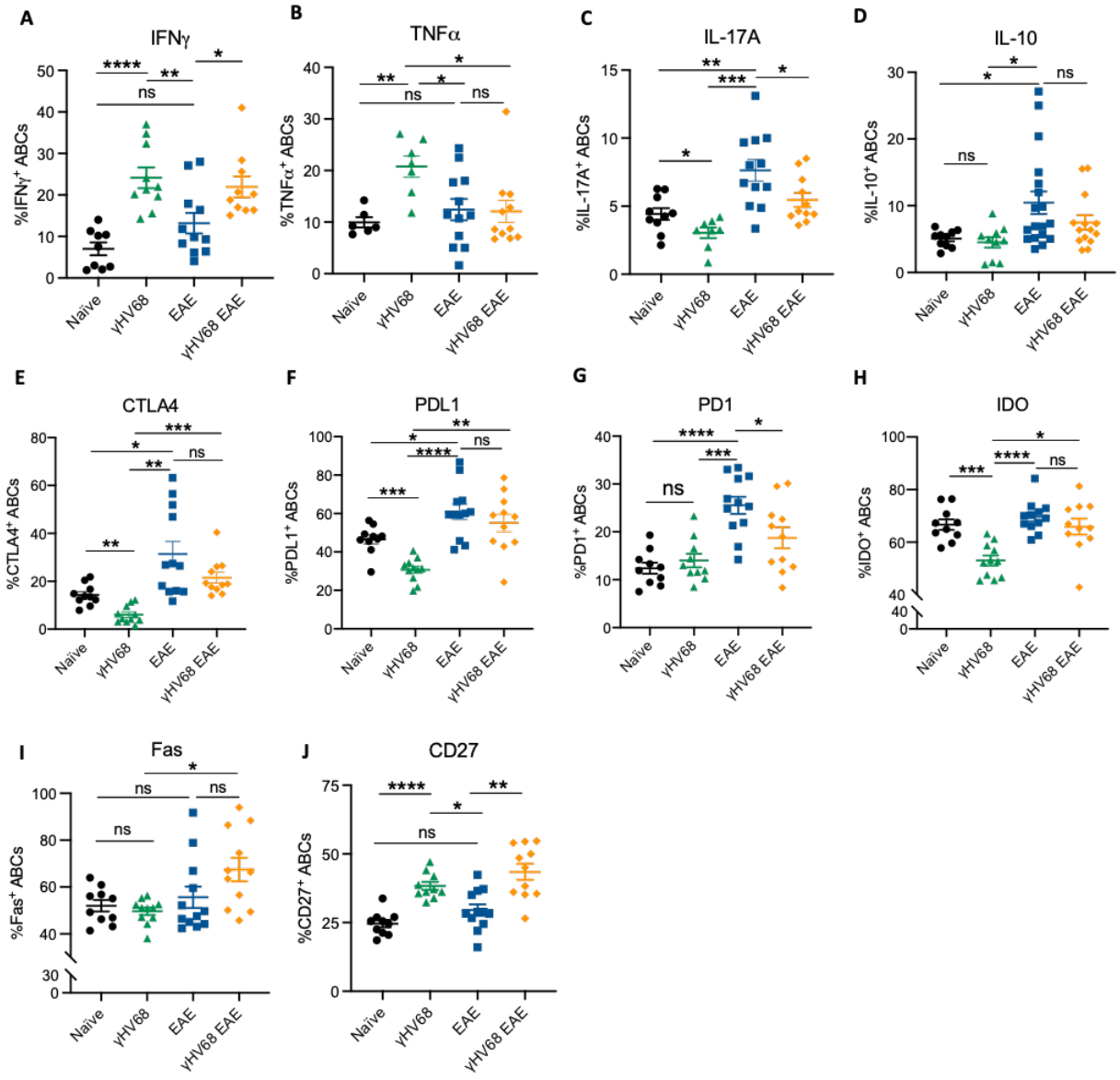

761

762 **Supplemental Figure 3:** C57BL/6(J) mice infected with γHV68 for 35 days (γHV68, green

763 triangles) or mock-infected (naïve, black circles). In some mice, MOG_{35-55} EAE was induced 35

764 days after mock infection (EAE, blue squares) or initial infection (γHV68 EAE, orange diamonds).

765 At 35 days p.i. or 13 days post EAE induction, spleen was collected and processed for flow

766 cytometry. Percentage of ABCs ($CD19^+CD11c^+T\text{-}bet^+$) that are positive for (**A**) IFNγ, (**B**) TNFα, (**C**)

767 IL-17A, (**D**) IL-10, (**E**) CTLA4, (**F**) PDL1, (**G**) PD1, (**H**) IDO, (**I**) Fas/CD95, and (**J**) CD27. Data in each

768 graph are pooled across 2-3 experiments, n=9-18 per group. Data presented as mean ± SEM,

bioRxiv preprint doi: https://doi.org/10.1101/2021.07.22.453263; this version posted July 22, 2021. The copyright holder for this preprint (which was not certified by peer review) is the author/funder, who has granted bioRxiv a license to display the preprint in perpetuity. It is made available under aCC-BY 4.0 International license.

769 analyzed by one-way ANOVA with multiple comparisons, ****p<0.0001, *** p<0.001, **

770 p<0.01, * p<0.05.

bioRxiv preprint doi: https://doi.org/10.1101/2021.07.22.453263; this version posted July 22, 2021. The copyright holder for this preprint (which was not certified by peer review) is the author/funder, who has granted bioRxiv a license to display the preprint in perpetuity. It is made available under aCC-BY 4.0 International license.

771

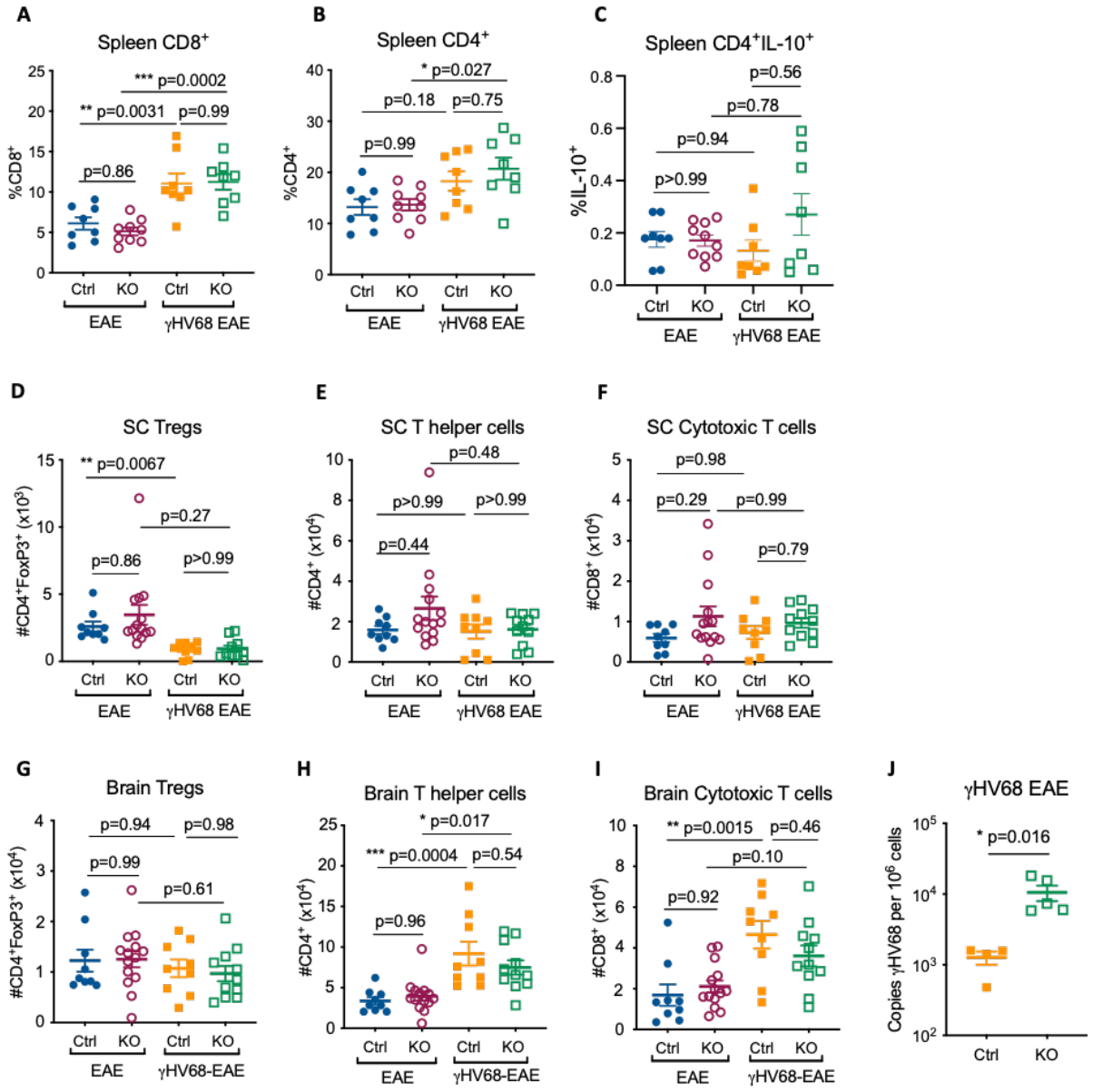

772

773 **Supplemental Figure 4:** Female *Tbx21*$^{fl/fl}$*Cd19*$^{cre/+}$ (KO) and *Tbx21*$^{fl/fl}$*Cd19*$^{+/+}$ (Ctrl) mice were

774 infected with γHV68 or mock-infected for 35 days and then induced for MOG_{35-55} EAE. At day

775 13-18 post-EAE induction spleen, brain, and spinal cord collected. Spleen, brain, and spinal cord

776 processed for flow cytometry and gDNA extracted from 4 x 10^6 splenocytes. (**A**) Percent

777 $CD3^+CD8^+$ (**A**) or $CD3^+CD4^+$ (**B**) of live lymphocytes in the spleen. (**C**) Percent of $CD3^+CD4^+$ T cells

bioRxiv preprint doi: https://doi.org/10.1101/2021.07.22.453263; this version posted July 22, 2021. The copyright holder for this preprint (which was not certified by peer review) is the author/funder, who has granted bioRxiv a license to display the preprint in perpetuity. It is made available under aCC-BY 4.0 International license.

778 in the spleen that are IL-10$^+$. (**D-F**) Total number, in the spinal cord, of CD45$^+$CD3$^+$CD4$^+$FoxP3$^+$

779 (**D**), CD45$^+$CD3$^+$CD4$^+$ (**E**), and CD45$^+$CD3$^+$CD8$^+$ (**F**) cells. (**G-I**) Total number, in the brain, of

780 CD45$^+$CD3$^+$CD4$^+$FoxP3$^+$ (**G**), CD45$^+$CD3$^+$CD4$^+$ (**H**), and CD45$^+$CD3$^+$CD8$^+$ (**I**) cells. (**J**) Copies of

781 γHV68 per 10^6 splenocytes, as determined by qPCR. Analyzed by one-way ANOVA with multiple

782 comparisons (**A-I**) or Mann-Whitney test (**J**), *** $p<0.001$, ** $p<0.01$, * $p<0.05$.